Polymers **2012**, *4*, 501-538; doi:10.3390/polym4010501

OPEN ACCESS

polymers

ISSN 2073-4360

www.mdpi.com/journal/polymers

Review

Synthetic Strategies towards Fullerene-Rich Dendrimer Assemblies

Uwe Hahn [1,*], Fritz Vögtle [2] and Jean-François Nierengarten [1,*]

[1] Laboratoire de Chimie des Matériaux Moléculaires, Université de Strasbourg et CNRS (UMR 7509), Ecole Européenne de Chimie, Polymères et Matériaux (ECPM), 25 rue Becquerel, 67087 Strasbourg Cedex 2, France

[2] Kekulé-Institut für Organische Chemie und Biochemie, Rheinische Friedrich-Wilhelms-Universität Bonn, Gerhard-Domagk-Strasse 1, D-53121Bonn, Germany; E-Mail: voegtle@uni-bonn.de

* Authors to whom correspondence should be addressed; E-Mails: uhahn@unistra.fr (U.H.); nierengarten@unistra.fr (J.-F.N.); Tel.: +33-368-852-764; Fax: + 33-368-852-774.

Received: 16 December 2011; in revised form: 1 February 2012 / Accepted: 8 February 2012 / Published: 14 February 2012

Abstract: The sphere-shaped fullerene has attracted considerable interest not least due to the peculiar electronic properties of this carbon allotrope and the fascinating materials emanating from fullerene-derived structures. The rapid development and tremendous advances in organic chemistry allow nowadays the modification of C_{60} to a great extent by pure chemical means. It is therefore not surprising that the fullerene moiety has also been part of dendrimers. At the initial stage, fullerenes have been examined at the center of the dendritic structure mainly aimed at possible shielding effects as exerted by the dendritic environment and light-harvesting effects due to multiple chromophores located at the periphery of the dendrimer. In recent years, also many research efforts have been devoted towards fullerene-rich nanohybrids containing multiple C_{60} units in the branches and/or as surface functional groups. In this review, synthetic efforts towards the construction of dendritic fullerene-rich nanostructures have been compiled and will be summarized herein.

Keywords: dendrimers; fullerene; nanotechnology; fullerodendrimers; self-assembly; supramolecular chemistry

1. Introduction

The conceptual design of dendrimers has been inspired by nature. The typical features of such macromolecules with multiply branched structures can be encountered for instance in the branching of trees and roots, but also blood vessels, nerve cells, corals, or snowflakes display archetypal fractal patterns. Though dendrimers have been described for the first time in the late 1970s [1], these highly symmetric and often spherical structures have only attracted increased attention throughout the last two decades. Whereas at the infancy of investigation on dendrimers fundamental research has been the driving force, the interest in recent years is nowadays more directed towards applications and core areas such as biology or medicine are clearly perceptible. The huge interest in dendrimers is strongly related to the capability of dendritic architectures to generate specific properties and functions, resulting from their unique molecular structures [2–4]. Another appealing characteristic of dendritic structures is the multiplication of functional groups at the periphery of a dendritic structure rendering possible the precise tuning of the materials properties.

Almost at the same time as dendrimer chemistry started to develop rapidly, Fréchet *et al*. presented the first dendritic specimens containing C_{60} as functional moiety [5]. Since then, the field of fullerodendrimers has generated significant research activities with new materials that exhibited intriguing properties [6–12]. Particularly, the peculiar physical properties of fullerene derivatives make fullerodendrimers attractive candidates for a variety of interesting features in supramolecular chemistry and materials science [9]. Emanating from the ball-shaped structure of C_{60} and the possibility of multiple functionalization, this versatile carbon allotrope has demonstrated its potential not only as a moiety at the center of the dendrimer structure, but also as functional unit at the surface of such branched structures. In this review, synthetic strategies and efforts for the preparation of fullerene-rich dendrimers have been compiled and will be summarized. The materials, properties and experiments conducted with the respective dendrimers will be briefly described but not discussed in depth.

2. Divergent Synthesis

The general principle of a dendrimer synthesis according to the divergent method proceeds stepwise from a multi-functionalized core building block, to whose reactive coupling sites are attached new branching units in the form of dendritic branches via a reactive terminal functionality [2–4]. Activation through for instance deprotection regenerates new reactive coupling sites for further branching units under creation of a new dendrimer generation with each branching unit. The iterative synthetic sequence progressively yields higher generations and permits the dendrimer to grow from the inside outwards. The divergent method makes attainable high-molecular nano-architectures, while at the same time, the exponential growth of the corresponding dendrimer structure may lead to structural defects since complete functionalization cannot always be ensured. Likewise, purification of structurally perfect from defective dendrimers often becomes tedious or almost impossible resulting from their very similar properties.

One of the key compounds in the preparation of fullerene-rich dendrimers has been C_s-symmetrical fullerene bis-adduct **1** (Scheme I). This functionalized fullerene derivative was obtained in ten steps according to a previously reported procedure [13]. Briefly described, it involved the synthesis of an

A_2B building block with two benzylic alcohol functions and a *t*-butyl-protected carboxylic acid function starting from dimethyl 5-hydroxyisophthalate. In contrast, 5-(hydroxymethyl)benzene-1,3-diol was reacted with long alkyl chains followed by the reaction of the residual alcohol moiety with *Meldrums'* acid. Fusion of the two precursors gave a bismalonate which was reacted under classical Bingel conditions with C_{60}, I_2 and 1,8-diazabicyclo[5.4.0]undec-7-ene (DBU) to afford carboxylic acid **1** after treatment with TFA. Importantly, the well-established strategy via 1,3-phenylenebis(methylene)-tethered bis-malonates produced regioselectively the *cis*-2 addition pattern at C_{60} [14]. Acid **1** has then been engaged in the preparation of well-defined fullerene-rich nanostructures as obtained by the divergent approach.

Scheme I. Synthesis of activated ester **1** and grafting to polypropylene imine (PPI) dendrimers **4-6** under the use of the divergent synthetic protocol.

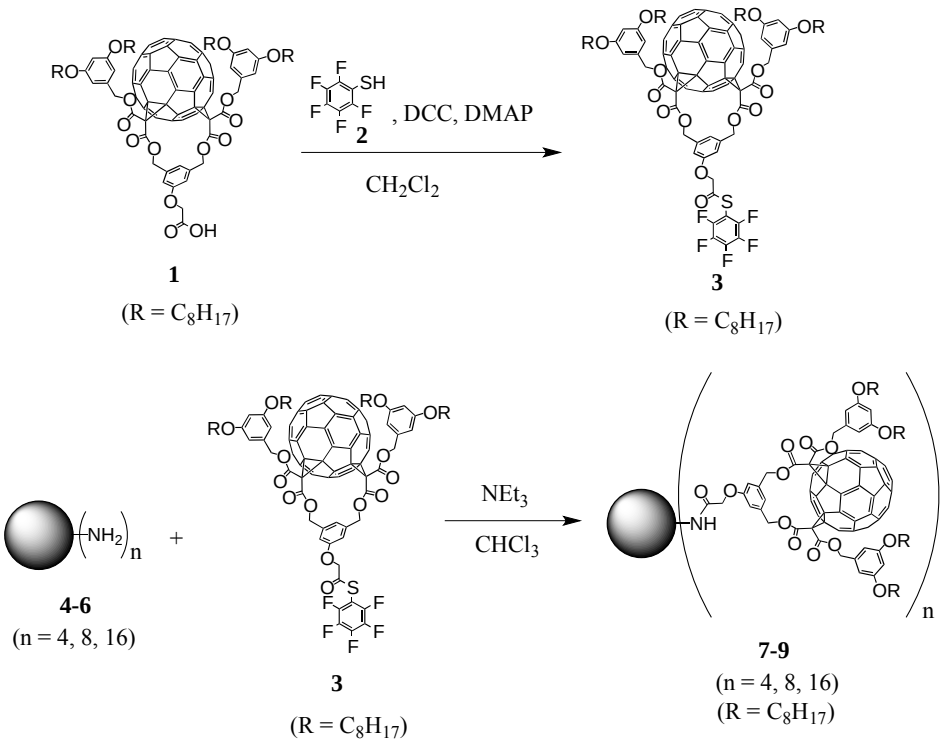

There are dendrimers available on the market like, e.g., polypropylene imine (POPAM or PPI) or polyamidoamine (PAMAM) dendrimers. In this first example of divergent preparation of fullerodendrimers, three generations with either 4, 8, or 16 surface amine groups have been used for decoration with a previously activated fullerene precursor (Scheme I) [15]. The choice of activation via pentafluorothiophenol ester **3** proved to be crucial for the functionalization. Owing to the nature of fullerene building block **1**, reaction conditions for the activation may not be strongly acidic or basic to preserve the ester functions. In addition, the ultimate step to graft the modified precursor to the multiple peripheral amines requires extremely efficient and high-yielding reactions to ensure complete functionalization without forming defected dendrimer structures. The corresponding pentafluorothiophenol ester **3** met these criteria as has been illustrated at various examples in the literature [16–18]. Accordingly, activated acid **3** was obtained in nearly quantitative yield upon reaction of carboxylic

acid **1** with pentathiofluorothiophenol **2** in the presence of dicyclohexylcarbodiimide (DCC) and a catalytic amount of 4-dimethylaminopyridine (DMAP). Subsequent reaction of the resulting activated ester with PPI dendrimers **4-6** of first to third generation using triethylamine as base provided the corresponding dendritic derivatives **7-9** in good yields (Figure 1).

Figure 1. Structures of fullerene-rich PPI-derived dendrimers **7-9**.

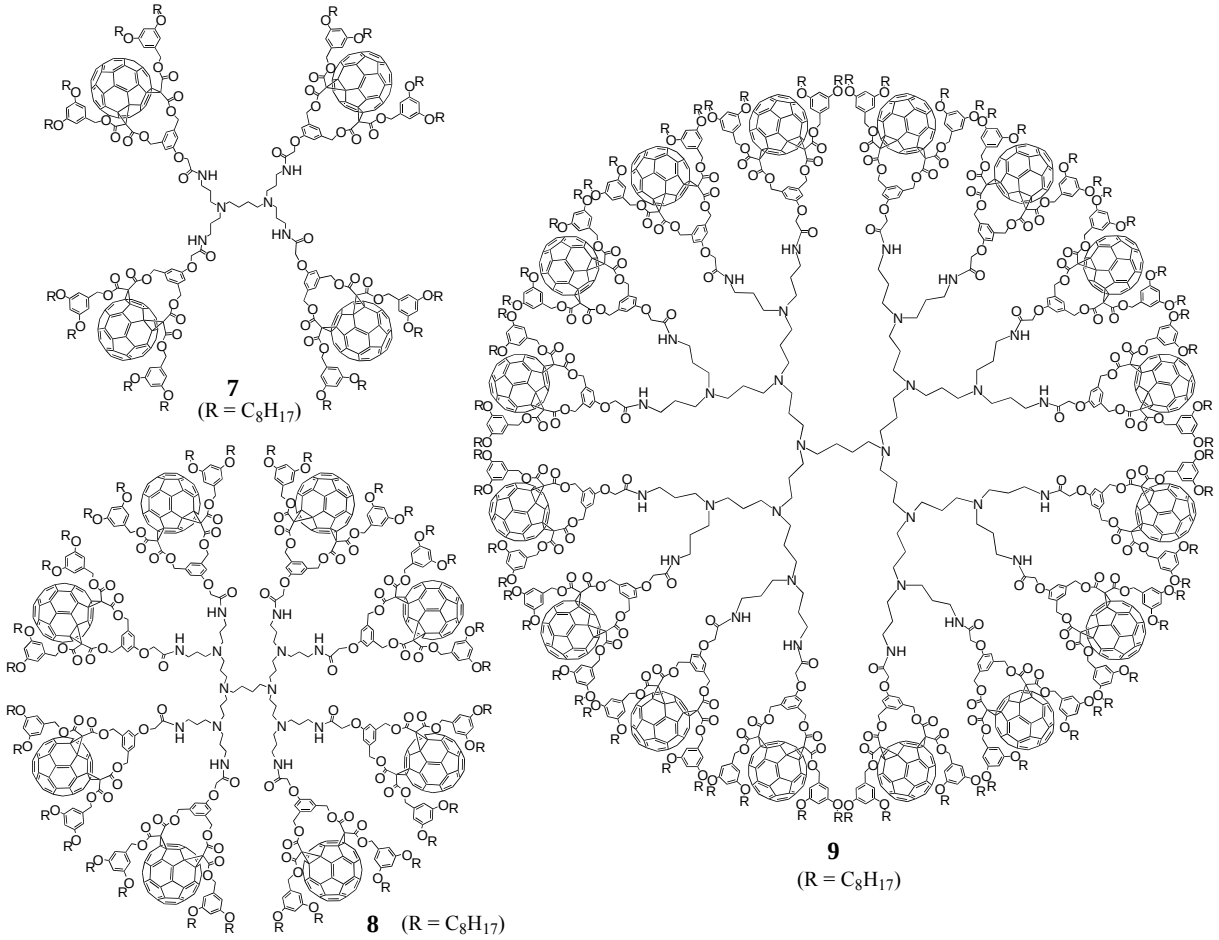

The fullerene-rich dendrimers are well soluble in a wide range of common organic solvents including CH_2Cl_2, $CHCl_3$, THF or toluene, due to the four pendant alkyl chains per C_{60} unit and spectroscopic characterization was easily achieved with the ^{1}H-NMR spectra of **7-9** to show the typical patterns of fullerene *cis*-2 bis-adducts and the expected additional signals arising from the PPI centrepart. Also MALDI-TOF mass spectrometry gave clear indication for the desired structures by depicting the expected molecular ion peaks. It is noteworthy that no peaks corresponding to defected dendrimers were observed in the mass spectra of **7-8**, thus providing clear evidence for their monodispersity. On the contrary, the spectrum for **9** showing a high level of fragmentation prevented the observation of the expected molecular ion peak and its monodispersity could not be unambiguously demonstrated.

Very recently, Wudl *et al*. presented a divergently grown dendronized norbornene derivative carrying four peripheral C_{60} moieties [19]. The synthetic protocol proceeded from a norbornene precursor bearing two terminal alcohol functions to which was reacted the anhydride of isopropylidene-2,2-bis(oxymethyl)propionic acid. After deprotection the four terminal hydroxyl

groups of **10** became accessible for attachment of 4-(2-ethylhexyloxy)-[6,6]-phenyl C_{61}-butyric acid. Initial attempts to couple both building blocks via DMAP-catalyzed [4-(dimethylamino)-pyridinium *p*-toluenesulfonate (DPTS)] esterification were not successful presumably due to steric hindrance between the acid functionality on the bulky fullerene cage and the peripheral alcohol groups in the dendron. On the contrary, conversion of the acid function into its acyl chloride **11** upon treatment with oxalyl chloride led to the target fullerodendron **12** (Scheme II). Polymerization of the exo-norbornene monomer was then carried out using the fast initiating third generation Grubbs' catalyst and the developed fullerene-rich linear polymer was claimed for possible applications in the field of polymer solar cells. Likewise, dendronized diblock copolymers have been reported [20]. However, incorporation of C_{60} units was attempted as the last step of the synthesis and did not lead to complete addition rather than a moderate coverage of approx. 50% of the peripheral long alkyl chains.

Scheme II. Synthesis of fullerene-rich norbornene-centred compound **12**.

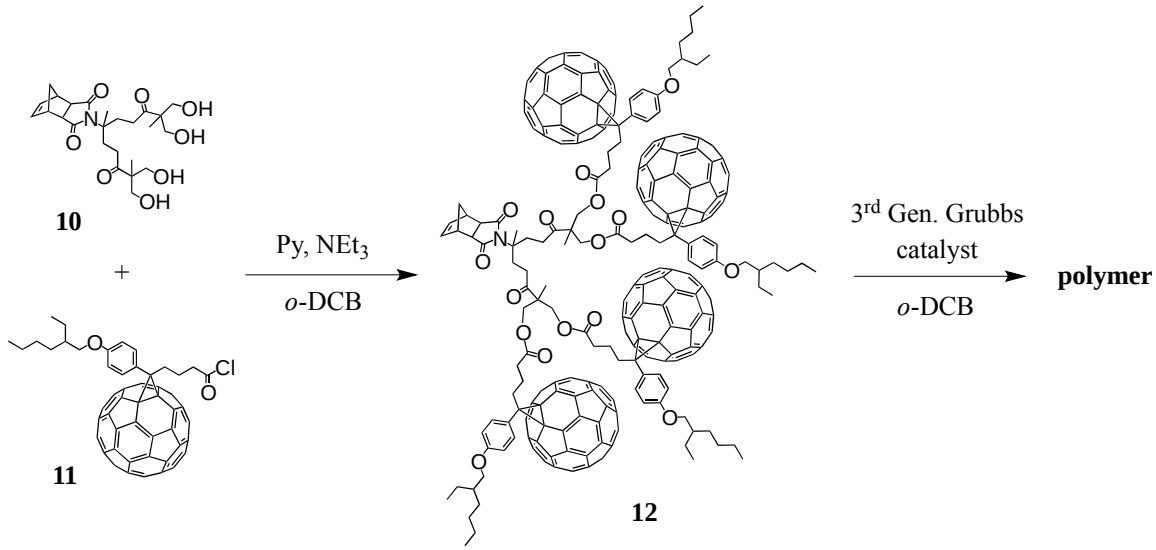

The group of Tomalia reported the preparation of a material containing a PAMAM dendrimer core coated with a shell of C_{60} molecules based on the known reaction of amines with the electron-deficient fullerene moiety in the presence of a base [21]. For this purpose, a large excess of fullerene has been dissolved in pyridine and it was slowly added a finely dispersed solution of G4 PAMAM dendrimer in pyridine. After stirring for one day and several purification steps, final material **13** was isolated in a 89% yield. As stated before, the reaction conditions as well as steric effects prevented complete derivatization hence obtaining a final product with a certain dispersity and a number of addends inferior to the total number of available primary amine groups, *i.e.*, 64. In addition, each fullerene could in principle react with more than one amine group as there were six independent pyracylene units per C_{60} molecule. Indeed, the authors studied the number of bonded C_{60} to the dendrimer surface in **13** by MALDI-TOF mass spectrometry and thermogravimetric analyses and it turned out that the results correspond to a C_{60}/dendrimer molar ratio of approximately 30:1. According to the authors, this number of almost exactly two terminal amine groups per fullerene suggests the bonding of two amine groups to most of the fullerenes (Figure 2). This material was used to catalyse photooxidation of thioanisole by generation of singlet oxygen. The oxidation reactions was found to occur in both

organic and aqueous solvents, with enhanced reactivity in aqueous solution, possibly due to a nanoreactor effect resulting from diffusion of hydrophobic reactant molecules into dendrimer cavities. Similarly, Godínez *et al*. deposited multilayer films of PAMAM generation 0.0 dendrimers and C_{60} on nanocrystalline TiO_2 electrodes to fabricate nanoassembled photoactive surfaces that absorbed in the visible region and offered a high molar extinction coefficient [22].

Figure 2. Proposed structure of **13** with covalently linked C_{60} at the surface of a polyamidoamine (PAMAM) G4-dendrimer.

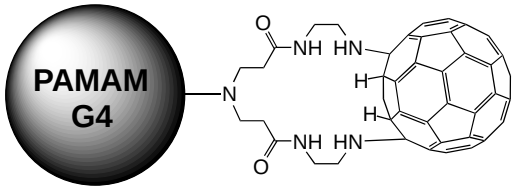

13

3. Convergent Synthesis

The convergent synthesis strategy proceeds in opposite direction, *i.e.*, from the periphery to the core. The main principle of this approach is the preparation of dendrons that are then grafted in the last step to a multifunctional core [1–3]. Repetition of the synthetic sequence again leads to the formation of different generations of fractal wedges that then ultimately furnish the dendrimer upon linking the dendrons covalently to the oligofunctional core moiety. Apart of the ease of purification due to very different weights that are often found for starting material and products, the most important feature of this approach is probably that structural monodispersity can be achieved. However, steric hindrance for the final coupling reaction might have a significant impact on the yield of the final dendrimer.

3.1. Dendrons

The first examples of dendritic branches containing several fullerene subunits have been reported by Nierengarten *et al*. starting from **1** as key building block [23] The iterative reaction sequence used for the preparation of the subsequent dendrimer generations was based on successive cleavage of a *t*-butyl ester moiety under acidic conditions followed by DCC-mediated esterification reactions with A_2B building block **14** possessing two benzylic alcohol functions and a protected carboxylic acid group in the presence of catalytic amounts of DMAP and hydroxybenzotriazole (HOBt). Subsequent cleavage of the *t*-butyl ester group of **15** was accomplished upon treatment with an excess of trifluoroacetic acid (TFA) in CH_2Cl_2 afforded G2 acid **16**. Repetitive esterification coupling with x and treatment with TFA gave **17** and **18**, respectively (Scheme III). Similar to the virtually quantitative yields for deprotection, the esterification steps under formation of generation two and three dendritic branches could also be obtained in excellent yields of 90 and 95%, respectively. The whole series of compounds can be easily obtained on a multi-gram scale and show good solubility in common organic solvents owing to the presence of the four long alkyl chains per fullerene moiety. As part of the research on functionalized dendrons, the coupling of the three generations of fractal structures **1**, **16**,

and **18** to a tris-isocyanante core has been described. Deposition onto gold electrodes revealed electron transfer from the electrode to the C_{60} subunits through space at a short distance from the electrode [24].

Scheme III. Preparation of fullerodendrons **16** and **18** of second and third generation.

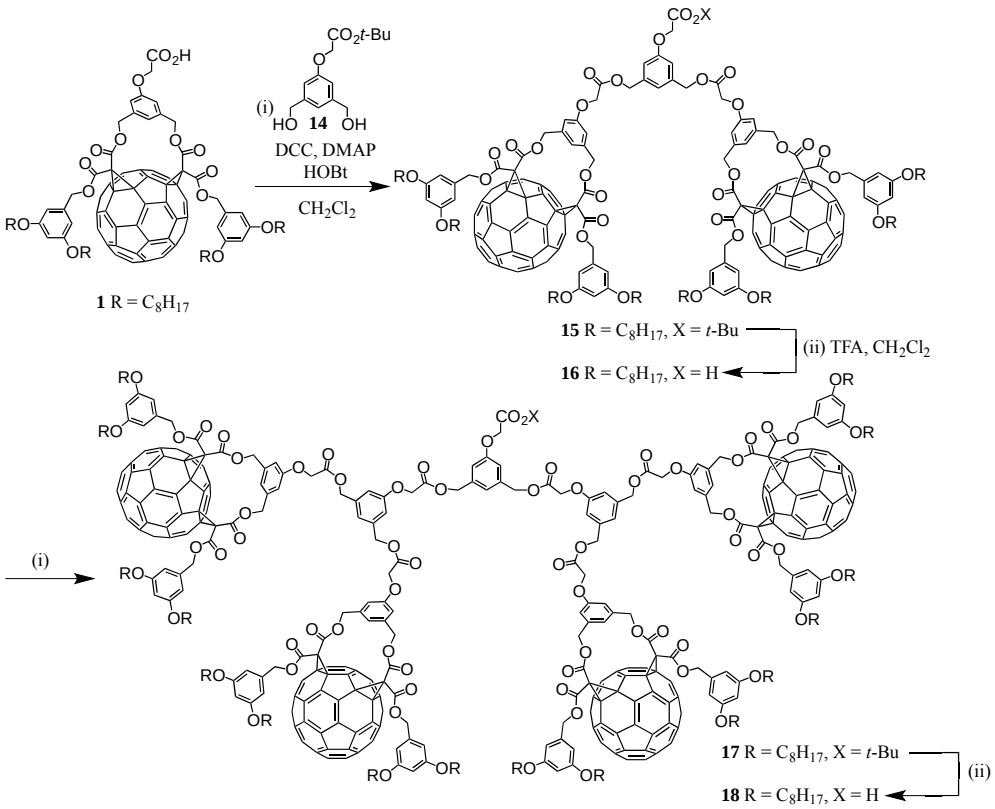

In continuation of their research on fullerene-containing dendritic branches and as a modification of the before used bis-addition pattern on the C_{60} sphere, the same group reported on methanofullerene derivatives that have been used as building blocks for the construction of dendrons [25]. Consequently, a simple malonate has been synthesized containing again at one end a carboxylic acid masked as *t*-butyl ester. At the other end, the malonate has been functionalized by two long alkyl chains that confer solubility to the system. Upon reaction with pristine fullerene under formation of a methanofullerene using Bingel reaction conditions, the ester is cleaved under the use of TFA to provide **19** with the targeted acid function.

As key building block for dendritic growth, a branching unit **20** has been designed bearing at each end of the alkyl chains *p*-methoxybenzyl (PMB)-protected hydroxy functions [25]. The choice of appropriate protecting groups for the two alcohol groups in **20** proved crucial as deprotection conditions must not be acidic to preserve the *t*-butyl ester moiety and may not be basic to preserve the other ester functions. Furthermore, decomposition of C_{60} derivatives under reaction conditions using fluoride prevented the use of silyl protecting groups. The PMB protecting groups in **20** could be removed with 2,3-dichloro-5,6-dicyanobenzoquinone (DDQ) in CH_2Cl_2 containing a small amount of water at room temperature. Under these neutral conditions, all the ester functions remained unchanged and compound **21** was thus obtained in a good yield of 84%. Reaction of acid **1** with diol **21** under classical Steglich esterification conditions allowed us to obtain *t*-butyl-protected second generation dendron **22** in 70% yield (Scheme IV). Subsequent quantitative cleavage of the *t*-butyl ester group with

TFA afforded acid **23**. Repetitive esterification/hydrolysis step thereby relying on the conditions as encountered for the lower generation dendrons, readily gave the respective third generation precursors **24** and **25**. All spectroscopic data were consistent with the proposed molecular structures. This molecule also served as scaffold to improve the reliability and the potential of the MALDI mass technique in the analysis of synthetic polymers and giant organic compounds [26].

Scheme IV. Preparation of fullerodendrons **23** and **25**.

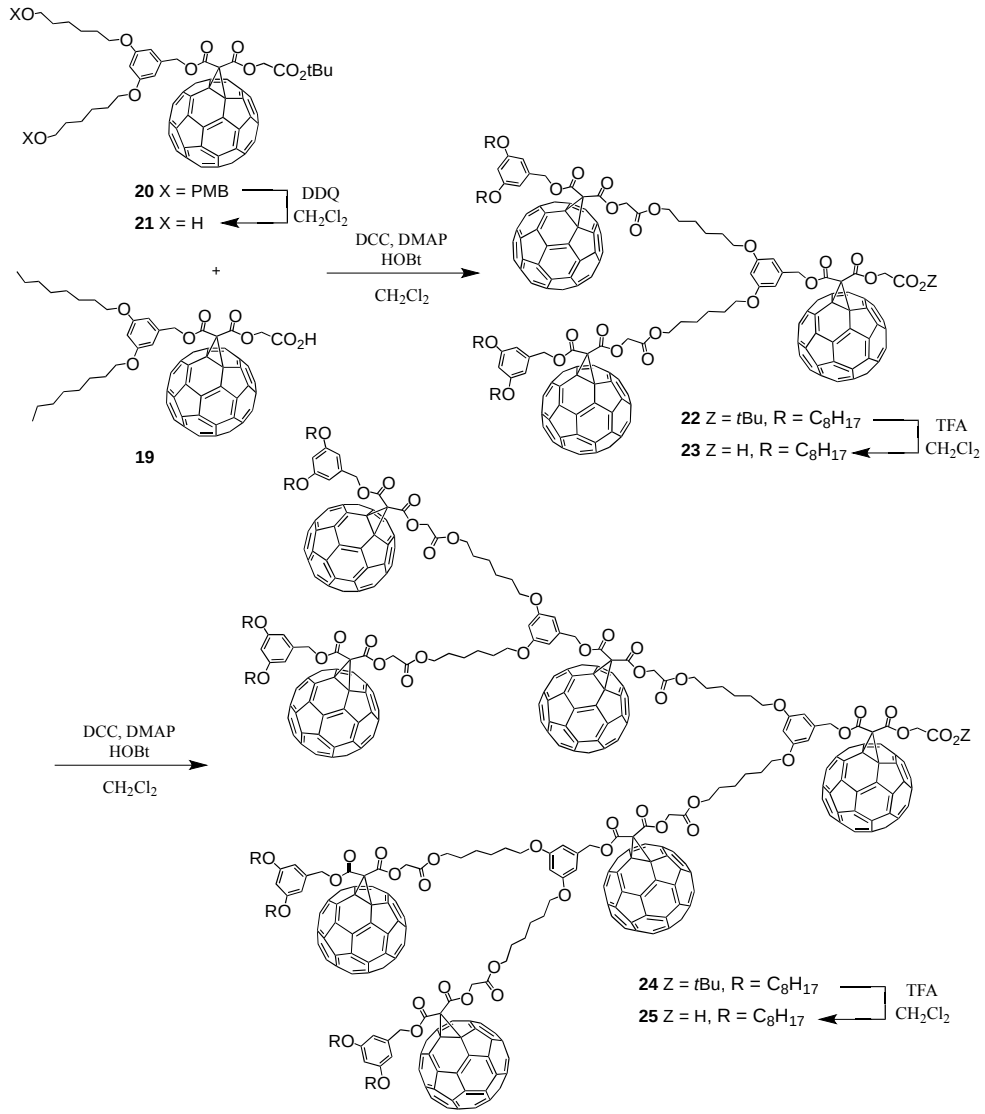

In a variation, also bis-Bingel adduct **26** has been equipped with four terminal hydroxyl functions using PMB as protecting group. To this end, carboxylic acid **1** was grafted under conventional esterification conditions to give pentad **27** whose *t*-butyl ester was hydrolyzed using TFA to give **28** (Scheme V).

Scheme V. Preparation of pentad **28**.

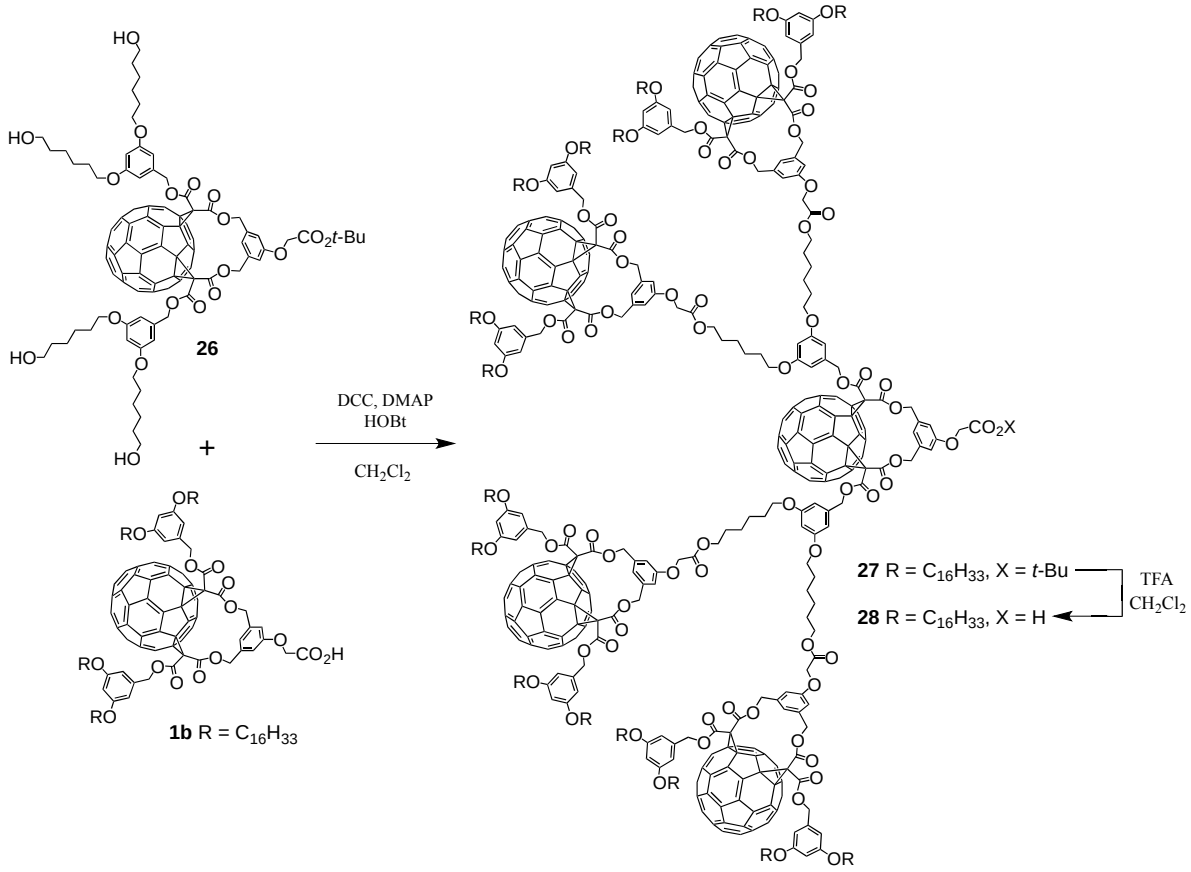

Amphiphilic fullerodendrons **1**, **16**, **18** and **28** have been demonstrated to display good quality Langmuir films at the air-water interface that can withstand pressures of up to 30 mN m^{-1} and cover extrapolated molecular areas at zero pressure up to 560 ± 30 $Å^2$ [27]. The authors also succeeded in forming Langmuir-Blodgett (LB) films by transferring monolayers of the whole series of four compounds onto solid substrates. However, the strong difference in size between hydrophobic and hydrophilic groups especially for the largest dendrons produces Langmuir films that are not sufficiently stable to stand the pressure over long period of time. This ultimately hampered the preparation of multilayered films.

The synthesis of high generation dendritic branches from building blocks **18** and **28** was found to be difficult mainly due to steric congestion. This prompted Nierengarten *et al*. to further explore the development of new fullerodendrons starting from a less hindered fullerene derivative (Scheme VI and VII) [28,29]. The iterative reaction sequence used for the synthesis of the dendritic branches up to fifth generation resembled the conventional protocol for repetitive esterification deprotection steps.

Scheme VI. Preparation of fullerodendrons **29-34** (Z = C_8H_{17}). *Reagents and conditions*: (i) TFA, CH_2Cl_2; (ii) DCC, DMAP, HOBt, CH_2Cl_2.

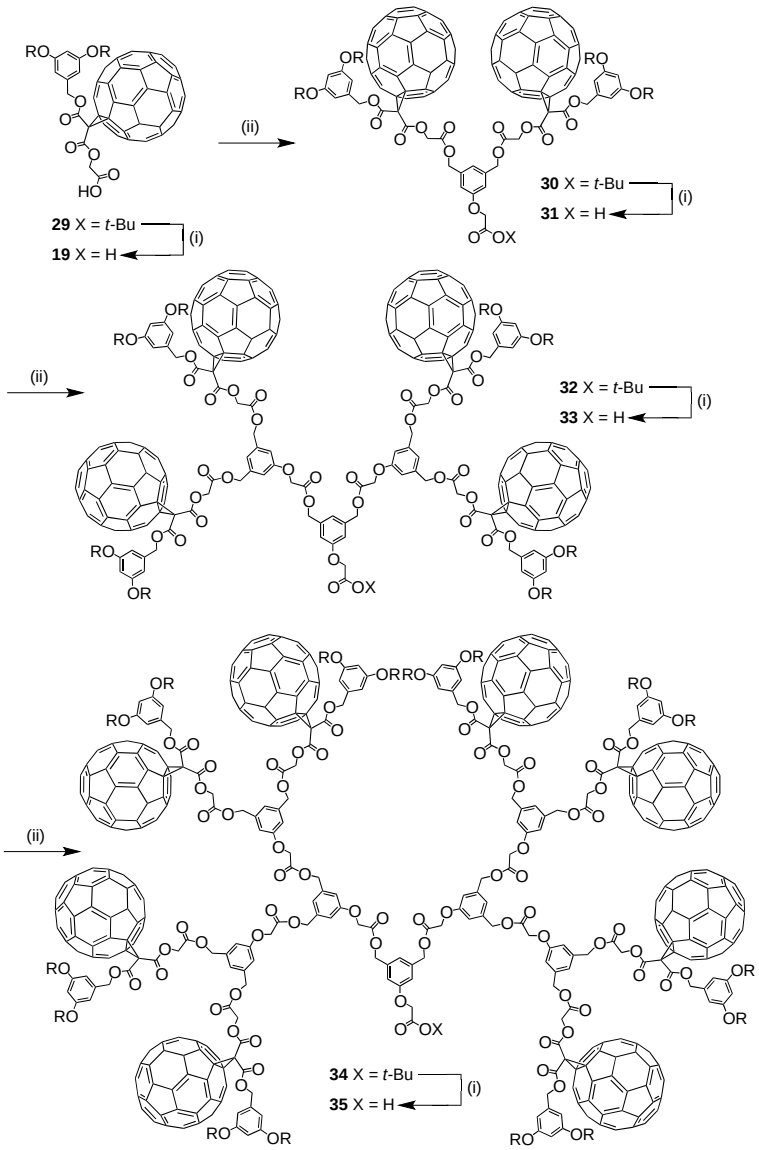

Correspondingly, reaction of acid **19** with diol **14** under esterification conditions (DCC, DMAP, HOBt) gave the protected dendron of second generation **30** in 90% yield. Hydrolysis of the *t*-butyl ester moiety under acidic conditions then afforded the corresponding carboxylic acid **31** in a quantitative yield. Esterification of **31** with diol **14** (DCC, HOBt, DMAP) gave **32** in 87% yield. Subsequent treatment with TFA afforded acid **33** in 99% yield. Reaction of **33** with diol **14** in the presence of DCC, HOBt and DMAP yielded fullerodendron **34** (95%), which after treatment with TFA gave **35** (97%). By repeating the same reaction sequence from **35**, the fifth generation derivatives **36** and **37** were also prepared (Scheme VII). The time needed to consume all the reactants during the esterification step was increased as the generation number grew. However, *N*-acyldicyclohexylurea by-products resulting from the rearrangement of the activated acid intermediates were quite limited even for the highest generation compound, thus allowing the preparation of the fifth generation protected dendron **34** under DCC-mediated esterification conditions in a good yield (76%). This synthetic methodology successfully mirrored the high efficiency for the preparation of fullerene-rich

derivatives **30**-**37**. These efforts thereby did not suffer from the reduced accessibility of the reactive group located at the focal point of the dendritic structure as observed for the first series of dendrimers synthesized under similar esterification conditions as described above. Structural elucidation by the NMR technique was easily achieved as all signals of the parts of the dendrons appear in different regions thus allowing the facile assignment of signals.

Scheme VII. Preparation of fullerodendrons **21-22** (R = C_8H_{17}). *Reagents and conditions*: (i) DCC, DMAP, HOBt, CH_2Cl_2; (ii) TFA, CH_2Cl_2.

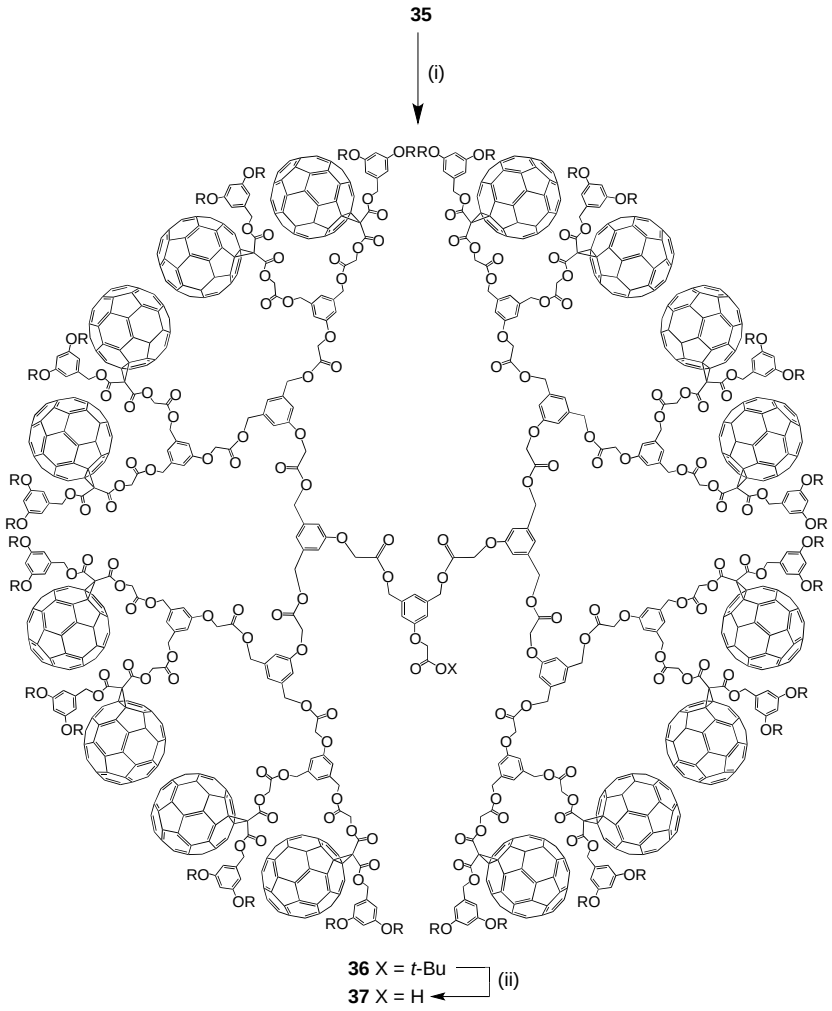

The whole series of *t*-butyl-protected dendrons have been subject of photoelectrochemical measurements. Preliminary experiments by injection of toluene solutions containing the appropriate dendron into acetonitrile resulted in the formation of large clusters in the solvent mixture [30]. The order of the mean diameters was not consistent with that of their molecular sizes ranging from 790 nm for $(\mathbf{29})_m$ to 90 nm for $(\mathbf{36})_m$. This phenomenon was explained by *inter*molecular interactions among branches that were prevalent thus leading to poorly packed dendrimer clusters with a large size, whereas for the larger dendron structures *intra*molecular interactions were dominating. Electrophoretical cluster deposition onto ITO/SnO_2 electrodes allowed the authors to obtain films that were composed of closely packed clusters with sizes in the range of 900 nm for **29** to 100 nm for **34** and **36**. Photoelectrochemical measurements gave photocurrent responses being prompt, steady, and

reproducible during repeated on/off cycles of visible light illumination. Incident photon-to-photocurrent efficiencies (IPCE) have also been studied reaching values of 1.7 % for ITO/SnO_2/(**29**)$_m$ and 6.0% for ITO/SnO_2/(**36**)$_m$ devices. The IPCE values turned out to be generation-dependent as displayed by increasing IPCE values along the series of dendritic clusters. Structural investigation on the fullerodendrimers revealed that the higher dendrimer generation were more densely packed clusters with a smaller, compact size (*vide supra*). The authors claimed that such fullerodendritic nanoclusters on ITO/SnO_2 in the higher generations would make possible to accelerate the electron injection process from the reduced C_{60} to the conduction band of SnO_2 via the more efficient electron hopping through the C_{60} moieties where the average distance between the C_{60} moieties is smaller.

3.2. Dendrimers

In connection with the before described fullerene dendrons that have been employed in Langmuir or LB films, the same group designed a more sophisticated system of amphiphilic character [31]. Carboxylic acid **28** containing five fullerene moieties was thus coupled to a polyethylene glycol terminated Fréchet-type dendron of third generation to give amphiphilic fullerene-rich dendrimer **38** (Figure 3).

Figure 3. Structure of amphiphilic fullerodendrimer **38**.

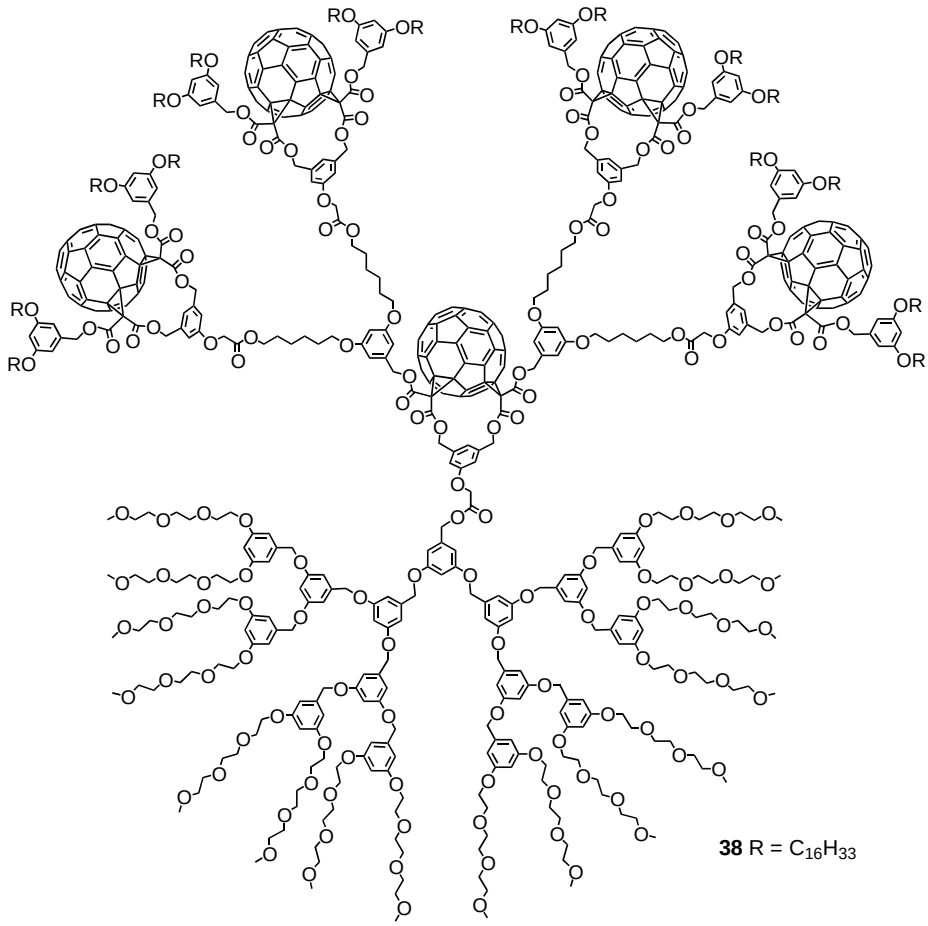

The diblock structure of dendrimer **38** exhibited a perfect balance between hydrophobic chains on one hemisphere and hydrophilic groups on the other to allow fabrication of stable Langmuir films that

were found to be reversible for successive compression/decompression cycles. In addition, transfer experiments of the Langmuir films onto solid substrates and the preparation of LB films were conducted for **38** leading to well-ordered structures on quartz slides or silicon wafers and multilayered LB films. The average layer thickness of approx. 36 Å indicated no or little interpenetration of successive layers.

The same dendritic precursors containing up to four C_s symmetrical fullerene bis-adducts in the outer sphere were then also used for grafting onto an oligophenylenevinylene (OPV) moiety previously modified by tetraethylene glycol chains [32]. DCC-mediated esterification at the two terminal hydroxylgroups with DMAP and HOBt as catalysts proved successful to readily provide OPV-centered dendrimers **39**-**41** (Figure 4). Systematic investigations of the photophysical properties of the whole series of dendrimers in different solvents evidenced singular polarity effects emanating from the dendritic structure. More specifically, the photoinduced electron transfer process from the fullerene singlet excited state has been found dramatically solvent dependent. In other terms, the energy of the charge separated state could be finely tuned around the energy value exhibited by the fullerene singlet excited state (~1.7 eV). In contrast, for the highest generation dendrimer, the strong solvent effects on the OPV–C_{60} charge separation processes were severely limited. By increasing the dendrimer size, electron transfer was progressively more difficult due to isolation of the central OPV core by the dendritic branches, which prevented solvent induced stabilization of charge-separated couples. Regardless of the solvent polarity, photophysical studies revealed ultrafast OPV→C_{60} singlet energy transfer taking place upon photoexcitation of the OPV core for the whole series of dendrimers. On the contrary, despite identical electroactive units as monitored by the quenching of the fullerene fluorescence, electron transfer occurred differently along the series. By increasing the dendrimer size, electron transfer became progressively more difficult and virtually no electron transfer from the fullerene singlet could be observed for **41** in CH_2Cl_2, whereas some transfer process could still be detected in the more polar PhCN. These trends exhibiting a dendritic effect were rationalized by considering increasingly compact dendrimer structures in more polar solvents [11]. This implied that the actual polarity experienced by the involved electron transfer partners, in particular the central OPV, was no longer that of the bulk solvent. This strongly affected electron transfer thermodynamics which became less exergonic and thus slower and less competitive towards intrinsic deactivation of the fullerene singlet state.

Dendritic precursors **1**, **16** and **18** also served as starting point for the fabrication of cyclotrimers consisting of a hexaphenylbenzene centre and up to 24 terminal fullerene units [33]. Pursuing the convergent route, (ethyne-1,2-diylbis(4,1-phenylene))dimethanol **42** has been prepared. The two alcohol functions were then used as anchoring point for first to third generation fullerene-containing dendrons **1**, **16** and **18** using classical esterification coupling chemistry (DCC/DMAP/HOBt) to yield the linear dumble-shaped derivatives **43**-**45** (Scheme VIII). The cyclotrimerization of the resulting dendronized bis-arylalkynes was then a perfect tool for the synthesis of even larger fullerene-rich dendritic architectures **46**-**48** [28].

Figure 4. Structures of oligophenylenevinylene (OPV)-centred fullerodendrimers **39**-**41**.

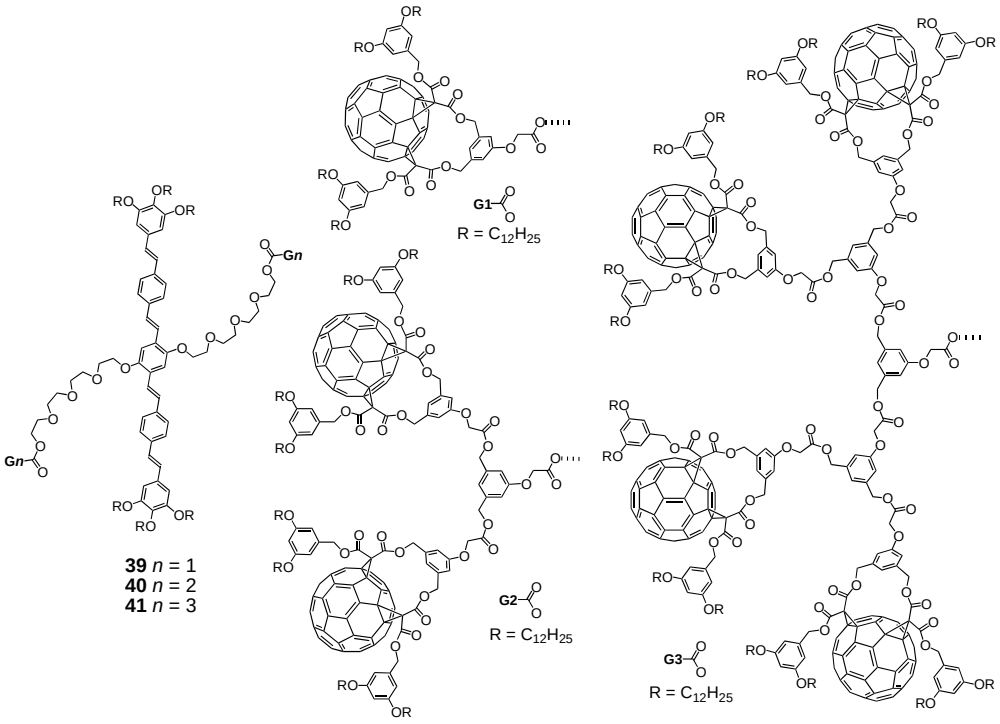

Scheme VIII. Schematic synthesis of fullerene-rich cyclotrimers **46**-**48**.

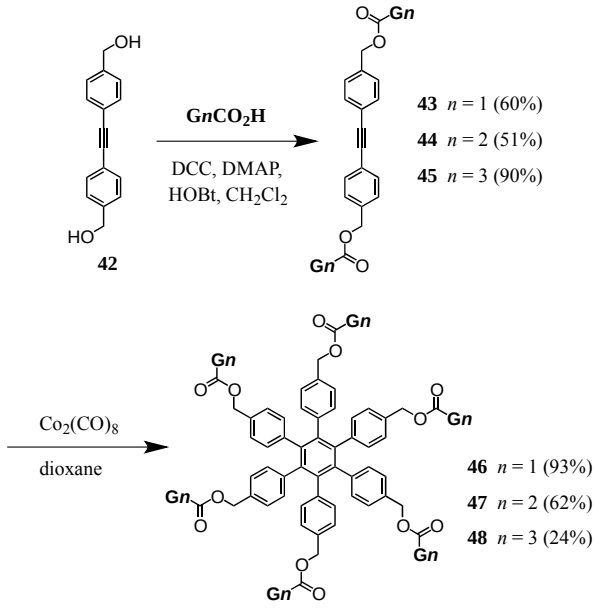

The reaction conditions for the cyclotrimerization were first optimized for the lowest generation alkyne **43**. The choice of $Co_2(CO)_8$ as catalyst was key to this synthesis. Indeed, it turned out that $Co_2(CO)_8$ efficiently catalyzed the cyclisation of three molecules of bisaryl alkynes under formation of a hexaphenylbenzene core. Under optimized conditions, treatment of **43** with a catalytic amount of $Co_2(CO)_8$ in dioxane at room temperature for 24 h afforded **46** in 93% yield. The same conditions were then used for the preparation of the higher generation compounds. The reaction of the second generation derivative **44** was finished after one day and compound **47** was isolated in 62% yield. In contrast, the reaction of the highest generation precursor **45** was very slow, most probably as a result of

steric effects. After 5 days, the starting material was not completely consumed but the reaction was stopped since notable degradation was evidenced. After purification by column chromatography on SiO_2 followed by gel permeation chromatography, compound **48** (Figure 5) was isolated in 24% yield.

Figure 5. Representative structure of the largest G3 fullerodendrimer **48** deriving from the cyclotrimerisation of dumbbell-shaped bisarylalkyne **45**.

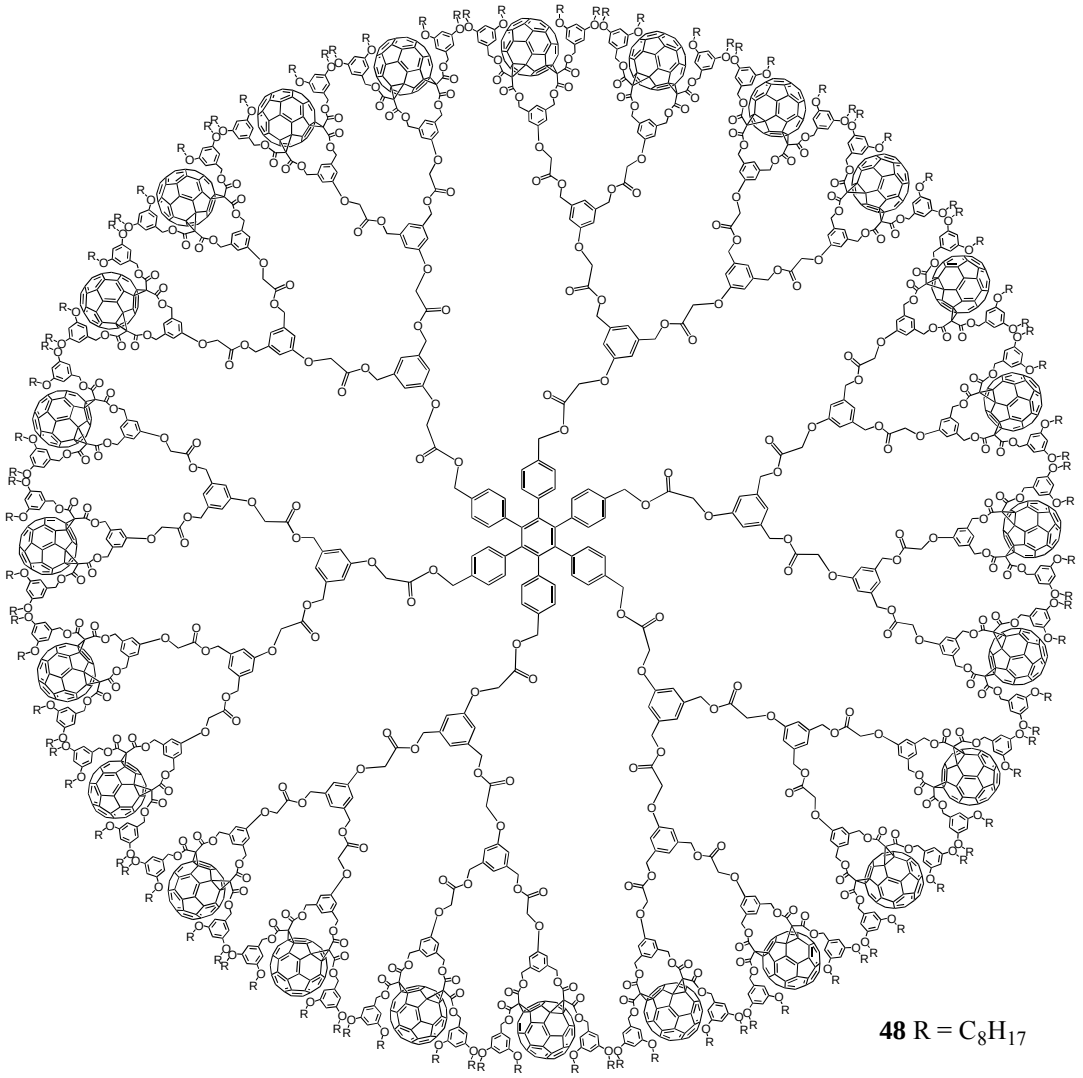

Very recently, the same group reported on fullerodendrimers with a perylenediimide central unit by a similar method as has been described before [34]. In first instance, a perylenediimide building block has been prepared following a three step synthetic protocol as decribed by Fréchet *et al*. [35]. The terminal hydroxyl groups were then again well suited for linking fullerene-containing dendrons **1**, **16** and **18** under formation of the first to third generation species **49**-**51** with up to eight peripheral C_{60} units (Figure 6). Electrochemistry clearly revealed that the oxidation of the dendrimers was centered on the perylenediimide core, while the first reduction always corresponded to a fullerene-centered process. Photophysical studies evidenced that there was generation-dependent behavior. However, though the lowest singlet levels of both photoactive components were virtually isoenergetic, a photosensitization process was observed for **49**-**51**. The fullerene triplet state was thus able to sensitize the lower-lying perylenediimide-centred triplet at a timescale of 10 ns making this system one of the

relatively rare examples of photoinduced energy transfer leading to long-lived triplet states centered on a dendrimer core and capable of sensitizing singlet oxygen.

Figure 6. Perylenediimide-centred first to third generation fullerodendrimers **49**-**51**.

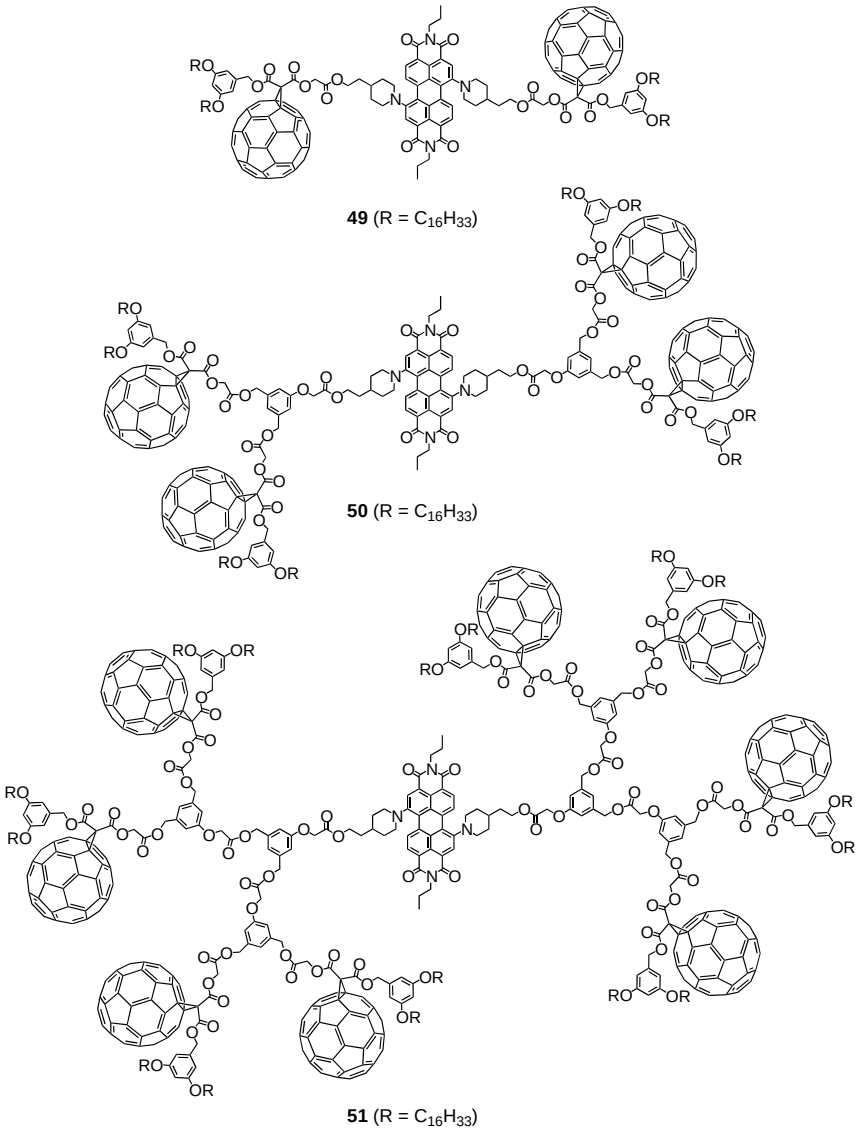

Another example of fullerene-rich nanoclusters has been described by Ito *et al*. consisting of multiple bis-Bingel C_{60} adducts that were associated with silicon phthalocyanines [36]. The synthetic route started with the preparation of a bis-functionalized fullerene precursor. The required bismalonate precursor equipped with a phenolic OH group and two long alkyl chains was obtained after four steps from the commercially available 5-hydroxyisophthalic acid. The macrocyclic bis-adduct was thus produced in 34% yield using the highly regioselective reaction developed by Diederich [37]. Reaction of two equivalents of the first generation precursors bearing a phenol moiety with silicon(IV) phthalocyanine (SiPc) dichloride proceeded smoothly in the presence of K_2CO_3 to produce the first generation triad **52** in 27% yield under formation of silicon-oxygen bonds (Figure 7). The key molecule for the construction of the next higher generations was 5-hydroxyisophthalic acid with a silyl-protected phenol group. The carboxylic acid groups were then involved in the Steglich esterification with G1 dendron to furnish the second generation upon deprotection of the silyl group

under the use of HF. Repetitive coupling/deprotection steps readily gave the third generation. Both dendritic branches were then coupled to the axial positions of SiPc to give the target dendrimers **53** and **54** in 62 and 25% yields as deep blue coloured solids (Figure 7). Studies by time-resolved fluorescence and transient absorption spectroscopy evidenced a generation-dependent charge-separation process from the SiPc to the C_{60} subunits with the lifetimes of the radical ion pairs to be prolonged upon going to the larger specimens. This was attributed to a possible electron migration among the C_{60} subunits.

Figure 7. Structures of dendritic fullerene-rich assemblies with a SiPc central unit.

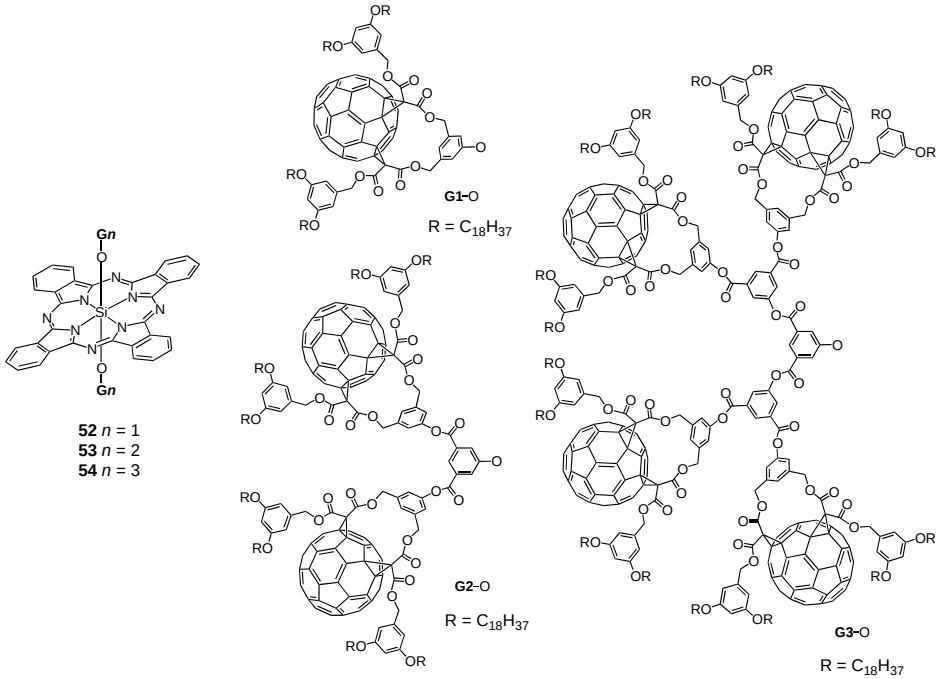

A challenging structure consisting of seven fullerene hexaadducts, one of which located at the center and the remaining six at the surface of the dendrimer, has been described recently by the group of Hirsch [38]. One of the key components was obtained from cyclo[2]octylmalonate which has been involved in the nucleophilic cyclopropanation of C_{60} under the use of CBr_4 and DBU to afford monofunctionalized Bingel adduct **55** in 28% yield. Within the next step, **55** was subjected to a 20-fold excess of bis-Boc-functionalized malonate **56** in the presence of 9,10-dimethylanthracene (DMA) and phosphazene base P_1-*t*Bu. Finally, the residual malonate group of [5:1]hexakisadduct **57** was engaged in the subsequent hexa-addition using again DMA and phosphazene base P_1-*t*Bu for the multiple Bingel cyclopropanation reaction and treated with TFA. This highly functionalized heptafullerene derivative **59** depicting a star-type architecture for the octahedrally functionalized C_{60} core had 60 positive charges at the surface, hence showing the expected high affinity towards water (Scheme IX). According to the authors, this multicationic architecture constituted the largest monodisperse molecular polyelectrolyte to date with defined three-dimensional structure that could find application in the field of (nonviral) gene delivery as the spherical shape resembled the globular shape of the natural DNA-histone complex.

Scheme IX. Synthesis of star-shaped heptafullerene polyelectrolyte **59**.

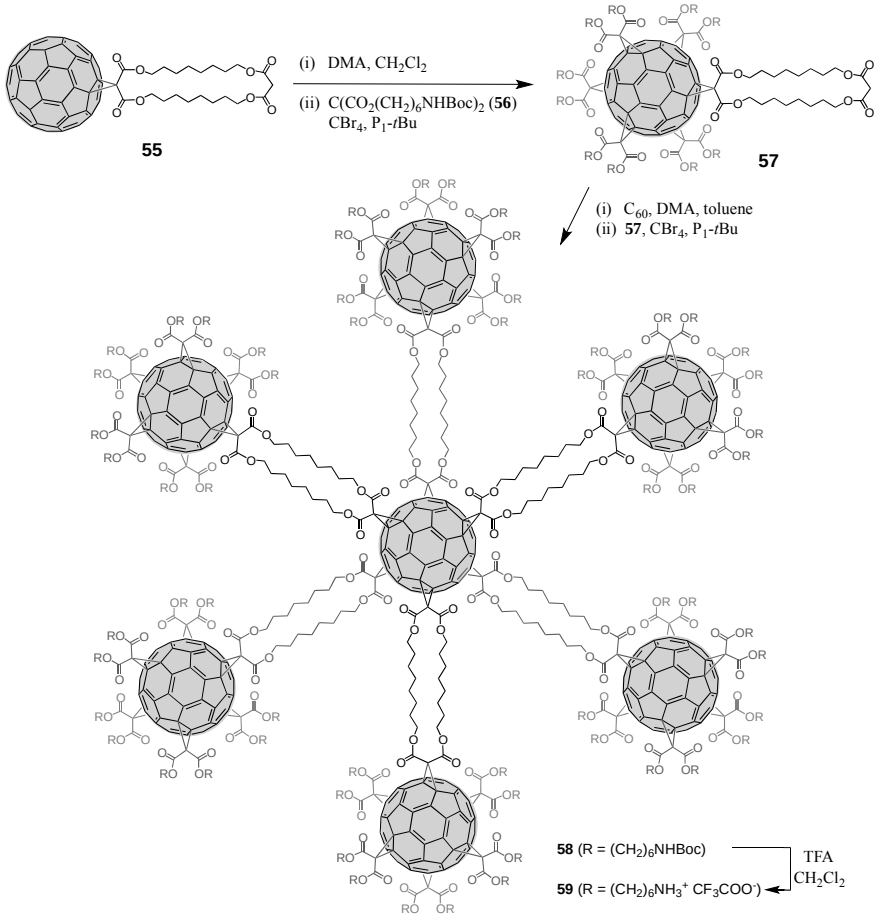

4. Molecular Self-Assembly of Fullerene-Containing Dendrons

The approach via self-assembly of dendrons using non-covalent interactions is particularly well-suited for the preparation of fullerene-rich macromolecules. Upon preparation of the dendritic branches the different moieties self-organize thus creating the dendritic macromolecular structure. This way, the often-encountered tedious final synthetic coupling reactions with a given multifunctional core can be avoided, as can problems regarding side reactions that may occur with potentially reactive functional groups like C_{60}. Nierengarten *et al*. exploited the self-assembly approach for the construction of organooxotin-derived clusters (Scheme X) [39]. Simple heating of an equimolar mixture of **19** and *n*BuSn(O)OH in benzene to reflux for 12 h using a Dean-Stark trap afforded the hexameric organostannoxane derivative **60** in 99% yield. The six tin atoms were chemically equivalent as well as the six trivalent oxygen atoms. The Sn–O framework of the molecule could be described as a drum with top and bottom faces each being comprised of a six-membered $(–Sn–O–)_3$ tri-stannoxane ring. The drum faces were joined together by six Sn–O bonds containing tri-coordinated oxygen atoms. The sides of the drum were thus comprised of six four-membered $(–Sn–O–)_2$ distannoxane rings, each of which was spanned by a carboxylate group that formed a symmetrical bridge between two tin atoms.

Scheme X. Preparation of first generation organooxotin cluster **60**.

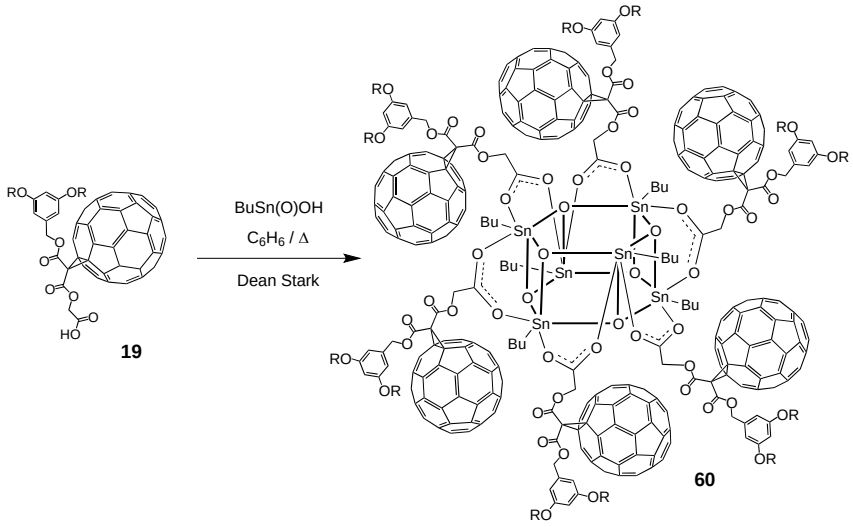

The optimized reaction conditions used for the preparation of **60** from carboxylic acid **19** were then applied to fullerodendrons **31** and **33**. The corresponding organostannoxane derivatives **61-62** were thus obtained in almost quantitative yields (Figure 8) [40]. Though the size of the dendron increased significantly upon going to generation three, the self-assembly process was not severely affected by the increased steric demand of the starting carboxylic acids with the close to quantitative formation of the final ensemble after 12 h. The latter observations were in contrast with previous findings as described before for which slow reactions and often only moderate yields were obtained for such third generation derivatives when compared to the corresponding first and second generation. Apart of the proton and carbon NMR spectra displaying the characteristic signals of the starting dendritic carboxylic acids and the expected additional resonances ascribable to the *n*-butyl chains, the respective ^{119}Sn NMR spectra brought final structural proof. The equivalence of all peripheral fullerene subunits as expected for a six-fold symmetric assembly with a drum-shaped organostannoxane core was found as a single ^{119}Sn resonance observed at *ca*. −480 ppm.

The use of metal coordination is perhaps the most widely developed method for the directed assembly of dendritic superstructures. In most cases, the metal center forms the core of the macromolecule, in which dendrons owing to their ligating groups at the focal point are able to be coordinated around a single, central metal ion. Nierengarten *et al*. used this method for the construction of large bis(1,10-phenanthroline)copper(I)-derived metal complexes **63-65** of first to third generation with up to 16 fullerene surface units (Figure 9) [41,42]. The synthetic procedure started from a modified 1,10-phenanthroline building block containing at the 2,9 positions pentanol groups. To these hydroxyl functions were then attached dendritic fullerene precursors **1**, **16** and **18** using classical DCC/DMAP/HOBt conditions. The dendritic ligands have thus been obtained in decreasing yields of 75, 48 and 24% yields. Treatment with $Cu(MeCN)_4BF_4$ in a 2:1 mixture of CH_2Cl_2/MeCN provided the target metal-based compounds **63-65** in good yields. However, due to problems during the purification process and the ionic metal complex character of the dendrimers, the isolated yields ranging from 56 for **63** to 33% for **65** were considerably lower as some material remained adsorbed on the column stationary phase. Structural elucidation by the NMR technique was easily achieved and clearly indicated complex formation by significant shifts of approx. 0.6 ppm as observed for the

methylene protons at 2,9 positions. From the electronic properties of dendrimers **63-65**, it could be deduced that the Cu(I) central core was strongly affected by the dendritic surrounding, *i.e.*, they were embedded in a *dendritic black box*. Whereas for the lowest generation **63**, oxidation of the central core was still possible though with lower amplitude, for the larger generation compounds **64** and **65**, oxidation was prevented by the large fractal branches. Furthermore, due to the increasing number of peripheral fullerene subunits in **64** to **65**, there was less and less light available for the core and the small portion of light energy able to excite the central Cu(I) complex was returned to the external fullerenes by energy transfer.

Figure 8. Fullerene-rich tin drum shaped clusters **61**-**62**.

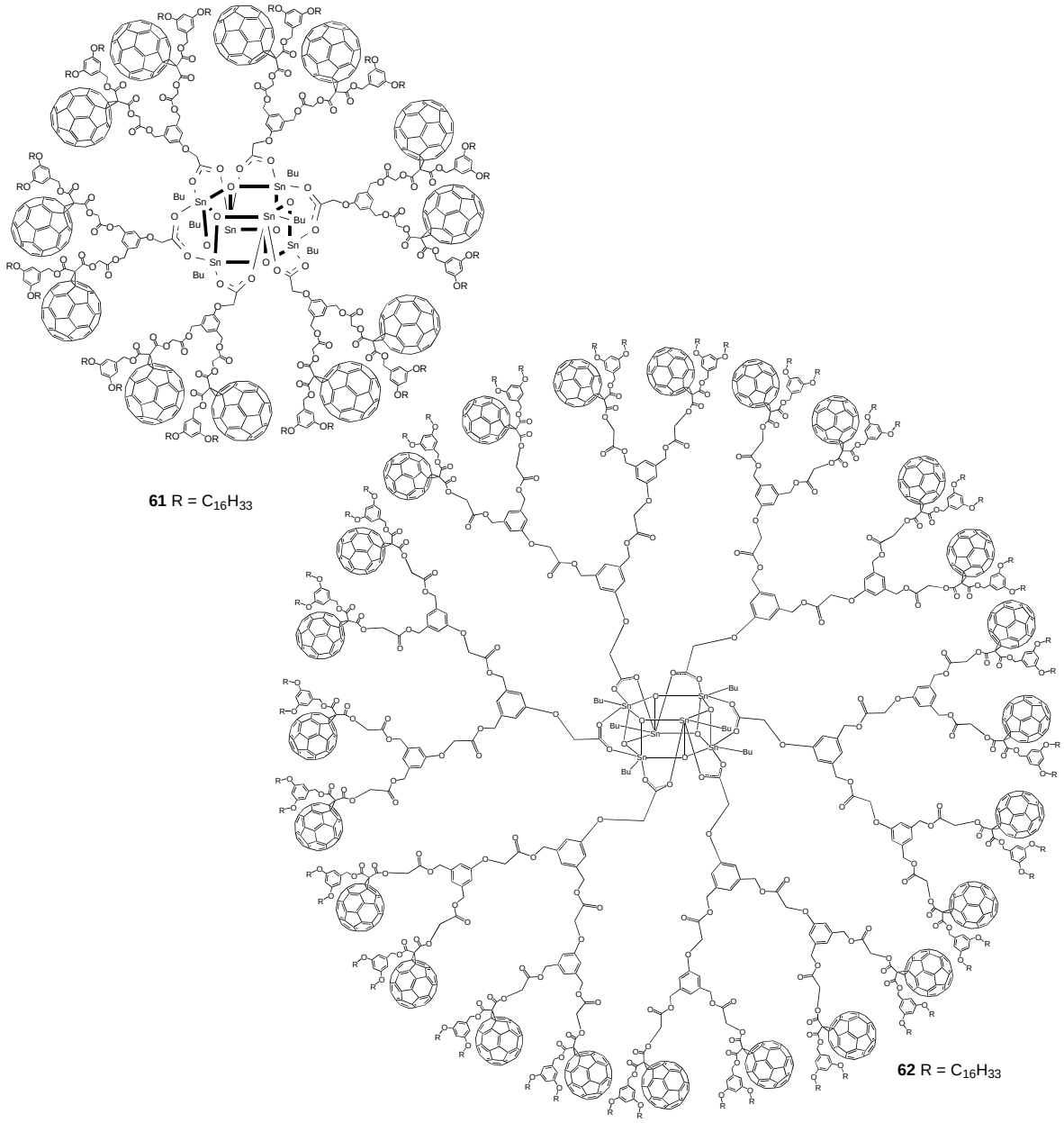

Figure 9. Structures of G1 to G3 fullerene-rich Cu(II) phenanthroline-based metal complexes **63**-**65**.

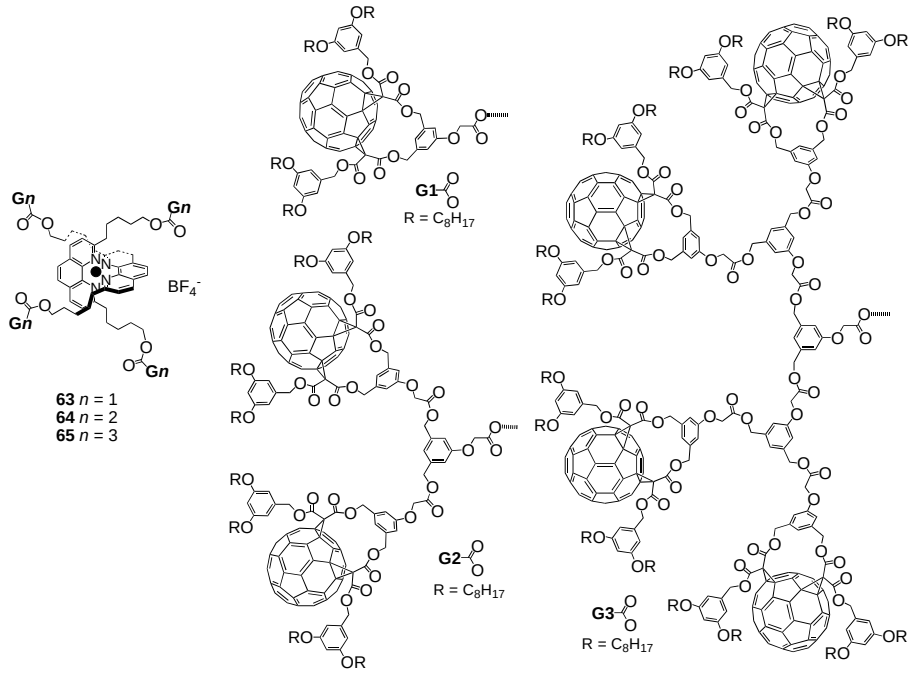

A key concept in supramolecular chemistry is the molecular self-assembly via hydrogen bonds. Such non-covalent interactions determine for instance the three-dimensional shape of proteins and nucleic bases. Presumably, the most important example constitutes the double helical structure of DNA that is largely due to hydrogen bonding between the base pairs upon linking one complementary strand to the other thus enabling replication. It is therefore not surprising that this concept has also been adopted in the preparation of fullerene-rich dendrimers. The group of Nierengarten *et al*. has indeed demonstrated that the self-assembly of dendritic macromolecules using hydrogen-bonding interactions was particularly well-suited to construct such macromolecular ensembles. In this nexus, supramolecular dendrimer $(\mathbf{69})_2$ has been obtained from the dimerization of a fullerene-functionalized dendron by a quadruple hydrogen bonding motif [43]. The self-complementary arrays of four hydrogen bonds, originally developed by Meijer *et al.*, afforded remarkably stable dimers with high association constants in apolar organic solvents (K_a 4 × 10^7 M^{-1} in $CHCl_3$) [44,45].

The required precursor namely a 2-ureido-4-[1H]pyrimidinone derivative bearing a residual Boc-protected amine function in position 2 and a 4-hydroxybutyl chain in position 6 has been obtained from diethyl 3-oxoheptanedioate following a three step procedure. To this end, dendrons **1** and **28** with either one or five C_{60} units and a focal carboxylic acid function have been coupled using standard esterification conditions (DCC/DMAP/HOBt). The resulting esters **67** and **70** have been obtained in 58 or 70% yield, respectively. Initial attempts to purify the first generation compound by typical column chromatography resulted in rather low yields of 30% thanks to partial cleavage of the Boc protecting group of the amine function in position 7. On the contrary, gel permeation chromatography proved to be more efficient hence yielding target substrate **67** in 58% yield. Similar purification conditions have then also been applied for building block **70**. The Boc-protecting groups of both dendrons were removed by treatment with an excess of TFA to afford amines **68** and **71** in good yields. Within the

final step of the synthetic sequence, the dendritic amines were subjected to reaction with octylisocyanate in the presence of triethylamine to give the desired supramolecular fullerene dimers $(\mathbf{69})_2$ and $(\mathbf{72})_2$ in yields of 48 and 87% (Scheme XI and XII).

Scheme XI. Preparation of supramolecular architecture $(\mathbf{69})_2$ resulting from the dimerization via quadruple hydrogen bonding.

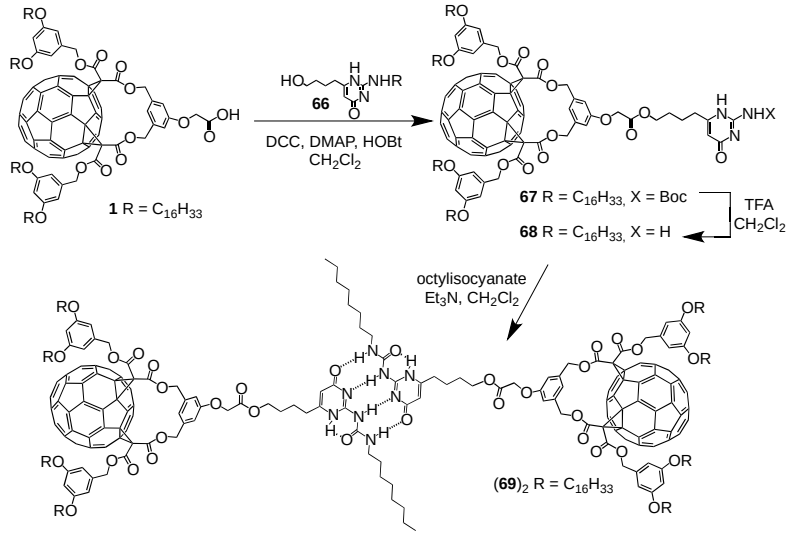

Spectroscopic characterisation via MALDI-TOF mass spectrometry indicated the formation of the proposed dimeric supramolecular structures. This technique, due to its mild ionization conditions and the concomitant marginal levels of fragmentations, was found to be a well-suited tool for characterizing such high-molecular-weight compounds. Even if the mass spectrum of $(\mathbf{69})_2$ was dominated by the ion peak corresponding to the monomer **69**, the molecular ion peak of dimer $(\mathbf{69})_2$ was also clearly detected. Similarly, in the MALDI-TOF mass spectrum of fullerodendrimer $(\mathbf{72})_2$ two peaks became apparent assignable to supramolecular dimer $(\mathbf{72})_2$ and to the monomeric structure **72**. These relatively low intensities as observed in the respective mass spectra could be easily rationalized by the rather weak non-covalent interactions. Nonetheless, the dimeric structures could be clearly detected and the absence of peaks corresponding to defected dendrons provided clear evidence for their monodispersity.

Definitive evidence for dimer structures of **69** and **72** could be deduced from the proton NMR measurements conducted in $CDCl_3$. For both dendritic assemblies, signals corresponding to single compounds were detected. Apart from the characteristic features emanating from C_s symmetrical 1,3-phenylenebis(methylene)-tethered fullerene *cis*-2-bis-adducts, and the additional typical signals from the different subunits of the modified fullerene precursors, large downfield shifts were found for the protons of the hydrogen-bonding motif. In both cases, the urea NH protons were found at $\delta = 11.8$ and 10.1 ppm and the intramolecularly chelated pyrimidinone NH at $\delta = 13.2$ ppm. This observation is fully consistent with four donor–donor–acceptor–acceptor (DDAA) hydrogen bonds in the supramolecular fullerene–dimer system.

Scheme XII. Preparation of supramolecular architecture $(\mathbf{69})_2$ resulting from the dimerization via quadruple hydrogen bonding.

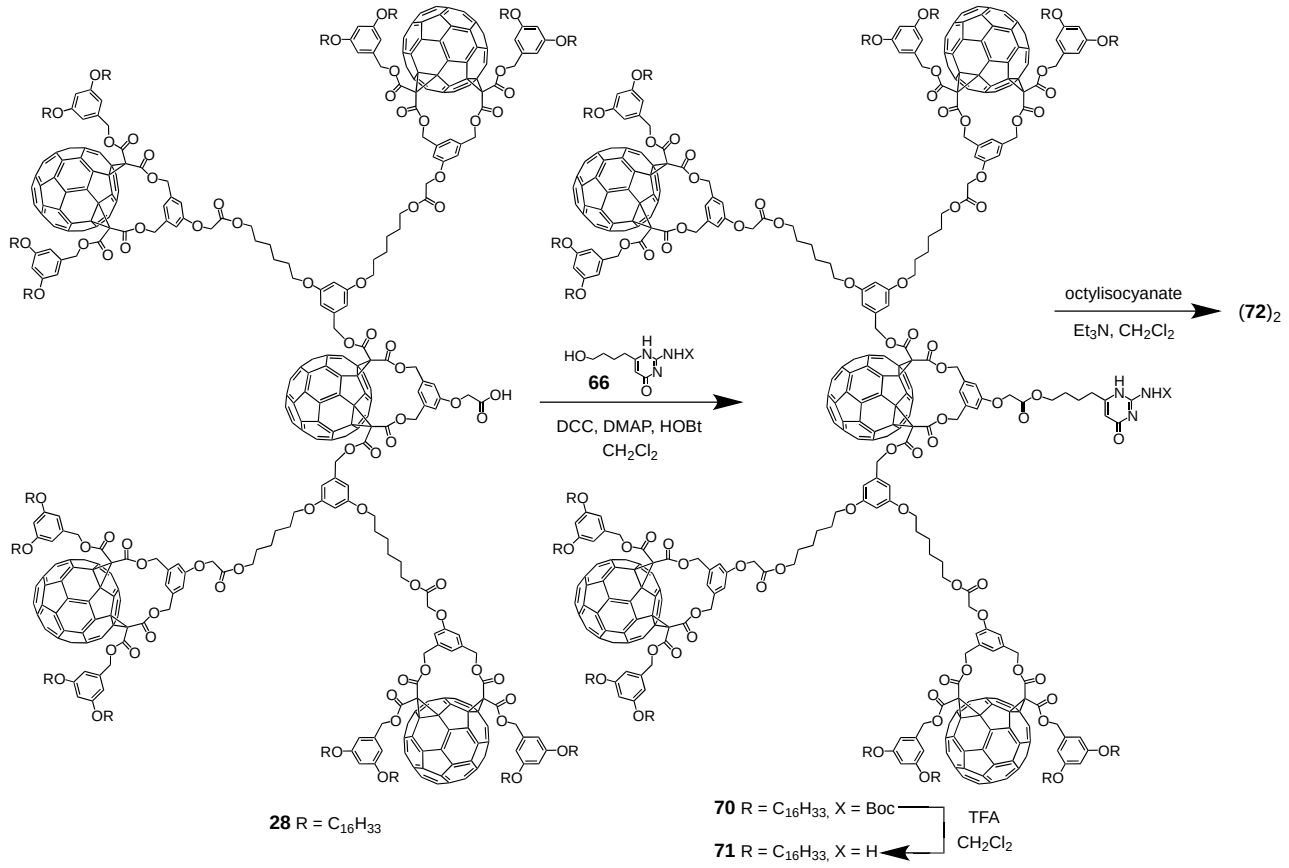

The ammonium–crown ether interaction is well-known in the field of molecular self-assembly. The diameter of the crown ether macrocycle largely determines the binding affinity under formation of host-guest complexes. One of the most prominent examples is 18-crown-6 that has a high affinity towards alkali ions such as potassium but is also famous to form quite stable complexes with protonated amines. Though the interactions are relatively weak for the latter case, they have been exploited for the association with fullerodendritic derivatives [46]. Correspondingly, ditopic OPV compound **73** has been equipped with two 18-crown-6 units (Figure 10). On the other hand, a Boc-protected amine has been coupled to fullerene dendron **1** using DCC/DMAP/HOBt. The final step then involved deprotection with TFA to readily afford the cationic ammonium trifluoroacetate salt **74** in 86% yield (Figure 10).

Figure 10. Structures of ditopic OPV host **73** and ammonium-containing dendrons of first to third generation **74**-**76**.

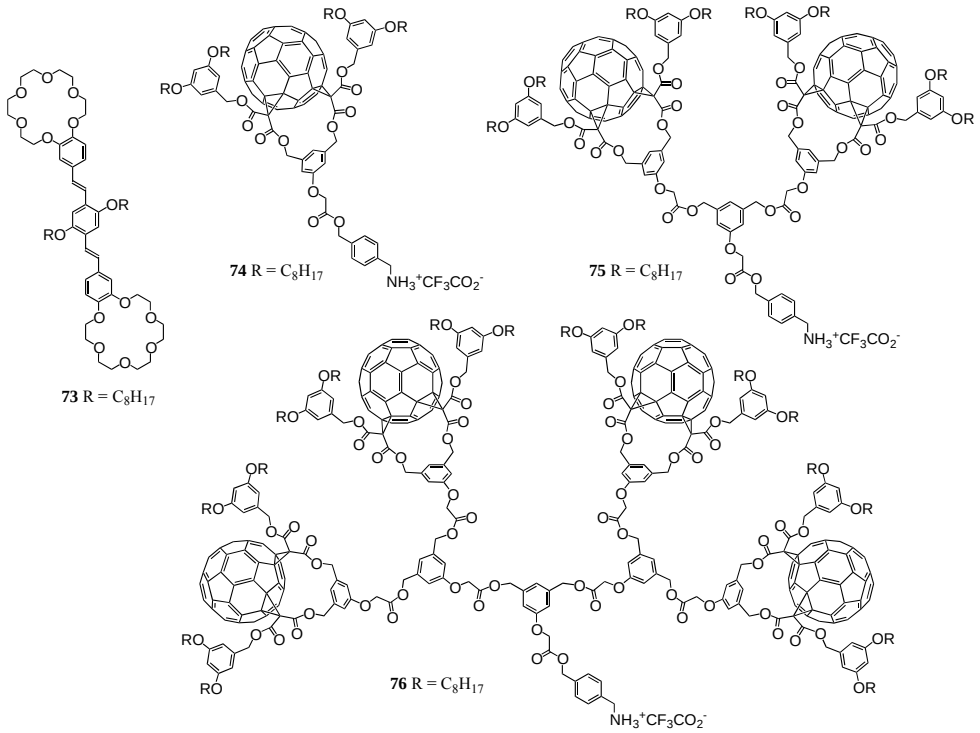

A mixture of compounds **73** and **74** self-assembled under formation of a stable 1:2 complex. UV/vis and fluorescence binding studies have been performed for the multicomponent photoactive devices in which the emission of the central ditopic receptor was dramatically quenched by the peripheral fullerene units. It turned out that the association constants were about one to two orders of magnitude higher than commonly observed for such systems, hence indicating additional recognition elements reinforcing the overall supramolecular structure. It was anticipated that favorable intramolecular fullerene–fullerene interactions were at the origin of this stabilization. Similarly, a two-center host–guest topography has been developed and it could be demonstrated that owing to the perfect complementarity of the two components, a bis-cationic substrate has been clicked on a ditopic crown ether derivative thus leading to a very stable non-covalent macrocyclic 1:1 complex [47]. As this approach appeared to be modular and easily applicable to a wide range of functional groups for the preparation of new supramolecular architectures with tunable structural and electronic properties, it has also been applied for the preparation of even larger dendritic nanoscale architectures (Figure 10) [48]. Accordingly, dendritic branches **16** and **18** were involved in the coupling to the same Boc-protected alcohol under the same conditions as conducted for **1** to yield the two cationic species **75** and **76** in good yields. Complexation with ditopic receptor **73** resulted in even enhanced binding constants thus displaying that there were even more secondary weak intramolecular interactions such as π-π stacking and hydrophobic interactions prevalent. These results mirrored another example for a remarkable positive dendritic cooperative effect. The authors emphasized that the size of the dendritic building blocks did not constitute a severe limitation for the self-assembly of large dendritic architectures.

Hirsch *et al*. used several (non-)dendritic mono-Bingel adducts for the self-assembly onto various Hamilton-receptor appended scaffolds via complementary hydrogen bonding [49]. Consequently, an

unsymmetric malonate has been functionalized under formation of ester bonds at one end with 3-bromo-1-propanol and on the other with *t*-butyl 4-hydroxybutanoate. The latter was subjected to hydrolysis and the free carboxylic acid employed in esterification reactions with different dendrons. Nucleophilic mono-cyclopropanation then readily produced the fullerene-containing dendritic wedges. Initial attempts to form the Bingel-adduct prior to the modification by dendrons were not successful. Within the last step of the synthetic sequence, the cyanurate moiety was introduced through reaction of the residual bromide function with cyanuric acid to produce the desired dendronized fullerene derivatives **77a-h**. Association studies with trivalent receptor **78** revealed a positive cooperativity, that originated from the preferably adopted planar *cis-cis* conformation rather than the other two possible topologies, *i.e.*, *trans-trans* or *cis-trans* (Figure 11). The authors also encountered a size-dependent behavior, *i.e.*, very voluminous ligands disfavoured the introduction of the second and third ligand due to steric demand. This effect was found more pronounced for Newkome and Fréchet-type dendritic substituents in **77a-b** and **77c-d**, respectively. In continuation of research in this field, the same group reported on the self-assembly of the depsipeptide-derived fractal branches **77e-h** onto different porphyrins to give photoactive supramolecular associates [50,51].

Figure 11. Supramolecular assemblies of monodendronized fullerene derivatives **77a-h** onto Hamilton-receptor functionalized host molecule **78**.

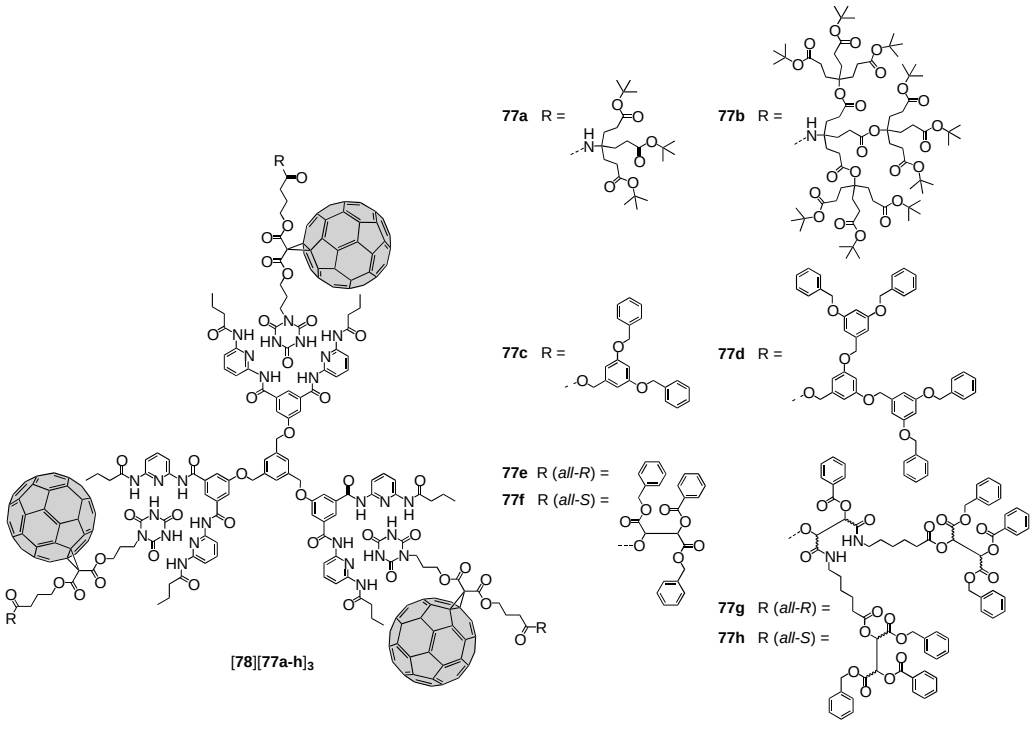

5. Molecular Self-Assembly of Fullerenes on Dendritic Scaffolds

Similar to the work of Tomalia as described above for the divergent functionalization of dendrimer backbones, pristine C_{60} itself could also been assembled on dendritic templates by using purely electrostatic interactions. Astruc *et al*. took advantage of the electrochemical properties of C_{60} to assemble a fullerene-rich supramolecular dendritic structure [52]. To an acetonitrile solution of one equivalent of dendrimer **79** consisting of a POPAM backbone and 64 peripheral ferrocene Fe(I) units

was titrated at −30 °C a toluene solution containing pristine C_{60}. After the addition of 64 equivalents of fullerene meaning a 1:1 stoichiometry, the deep blue greenish color of the ferrocene-modified POPAM dendrimer **79** disappeared, while leaving a black precipitate **[79][C_{60}]$_{64}$** whose proposed structure is depicted in Figure 12. This black-colored precipitate gave a clean quadrupole doublet for the Mössbauer spectrum whose parameters at 77 K were consistent with the presence of an Fe(II) sandwich complex. Its EPR spectrum recorded at 298 K shows the characteristic feature observed for a model compound obtained from the reaction of C_{60} with the 19-electron complex [Fe(I)Cp(η^6-C_6Me_6)]. The authors concluded a probable C_{60} reduction to its monoanion (Scheme XIII), as designed for a process that is exergonic by 0.9 eV. The peripheral cationic Fe(II) units with their C_{60}^- counteranion being very large, they were most likely located at the dendrimer periphery, presumably with rather tight ion pairs.

Figure 12. Fifth-Generation polypropylene imine (POPAM) dendrimer decorated with 64 ferrocene Fe(II)/($C_{60}^{\cdot-}$) ion pairs.

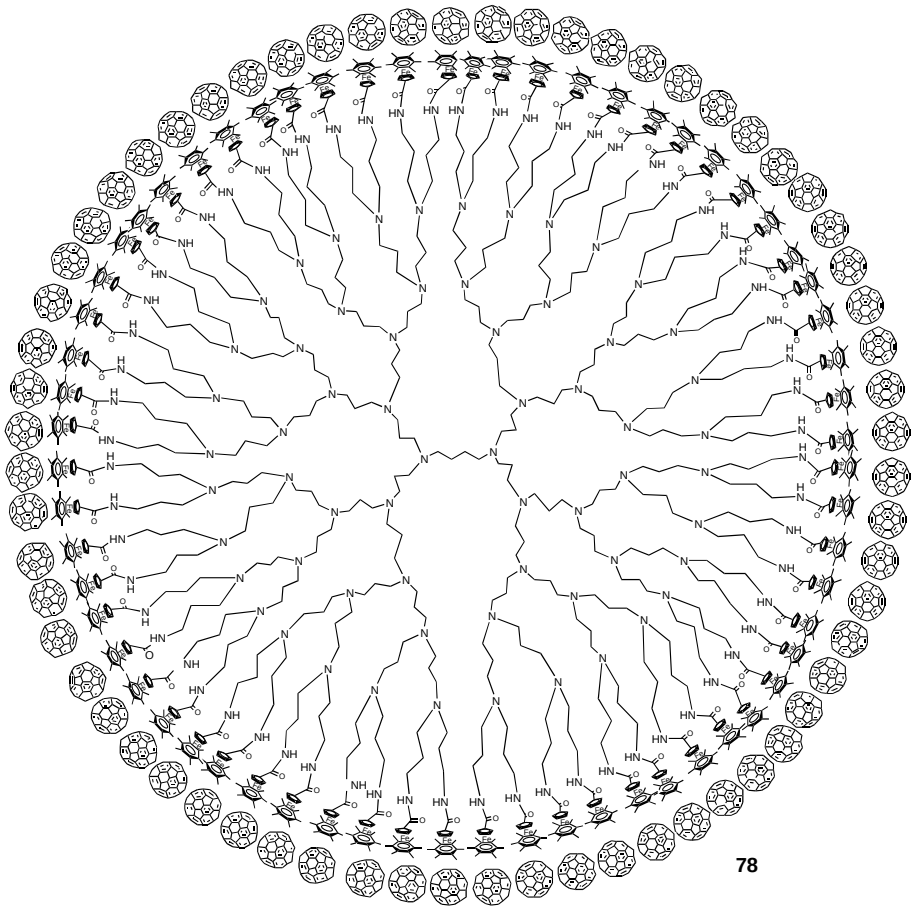

Scheme XIII. Electrochemical process accompanying the formation of the ferrocene-C_{60} ion pairs.

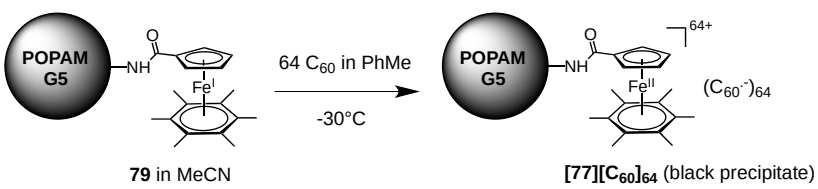

Another system based on electrostatic interactions has been reported by van Koten *et al*. [53]. A core-shell dendrimer with a cationic tetra[bis(benzylammonium)aryl] silane core has been used as a template for the assembly of fullerene-carboxylate derivatives via a straightforward anion exchange reaction of [**80**]Br_8 with Na[**81**] (Scheme XIV). In contrast to dendrimer **80**, the supramolecular fullerene-rich assembly [**80**][**81**]$_8$ was soluble in common organic solvents and its spectroscopic characterization could be easily achieved. In the ^{1}H NMR spectrum of a solution of [**80**][**81**]$_8$ in $CDCl_3$, the specific signals of both [**80**]$^{8+}$ and [**81**]$^-$ could clearly be observed. Furthermore, specific peak integrals showed that the octa-cationic dendritic moiety [**80**]$^{8+}$ and the anions [**81**]$^-$ were present in a 1 to 8 molar ratio. In order to establish the molecular weight of the host-guest assembly, gel permeation chromatography coupled to a low angle laser light scattering (GPC/LALLS) instrument was performed using THF as eluent. The chromatogram displayed three peaks. The first one corresponded to the 1:8 host-guest octa-fullero-dendrimer assembly [**80**][**81**]$_8$. The two additional peaks with higher molecular weights were assigned to superstructures consisting of aggregated assemblies derived from [**80**][**81**]$_8$. Such behavior was commonly observed during the GPC analysis of poly-ionic macromolecules when an organic solvent was used as eluent. Importantly, no peaks corresponding to compounds with a molecular weight lower than [**80**][**81**]$_8$ were detected, which further substantiates the formation of a stoichiometric assembly between octa-cationic [**80**]$^{8+}$ and eight [**81**]$^-$ anions.

Scheme XIV. Anion exchange reaction of [**80**]Br_8 with Na[**81**] leading to the fullerene-rich dendrimer [**80**][**81**]$_8$.

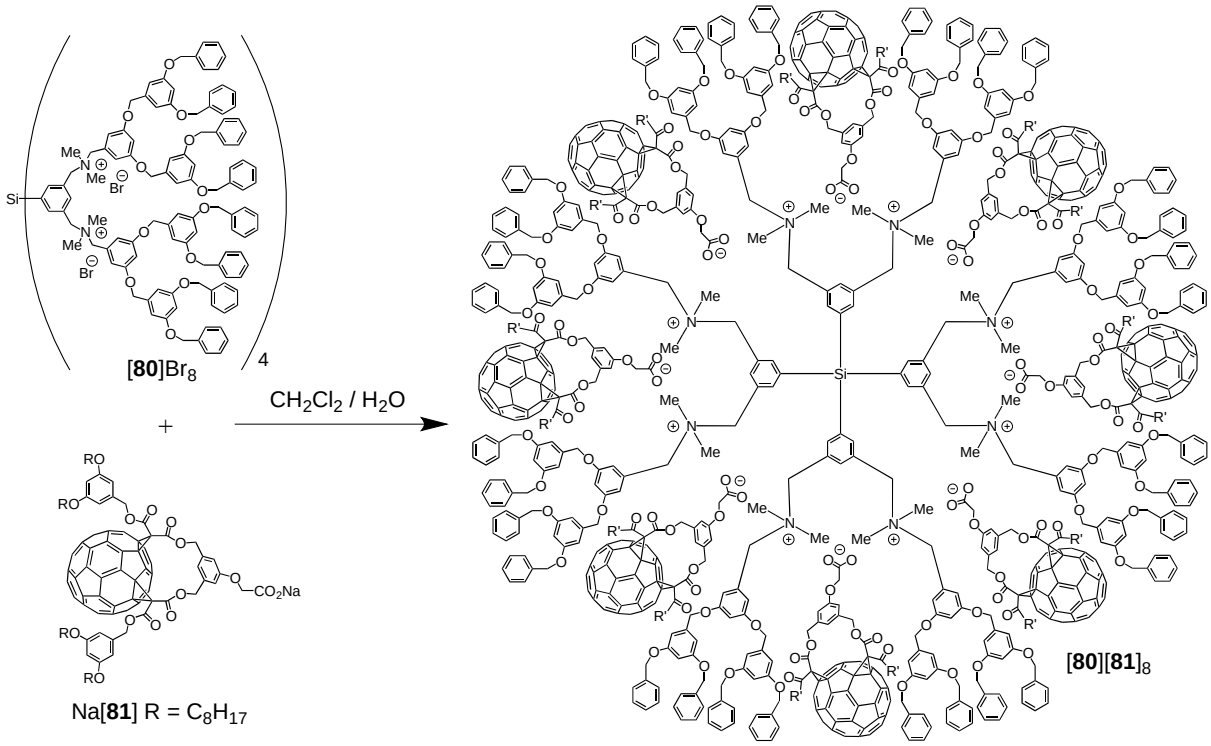

Aida *et al*. contributed to the field by introducing the metal-assisted coordination of modified fullerene derivatives to a multi-porphyrin dendrimer [54]. The synthetic protocol involved the preparation of a methanofullerene equipped with a long alkyl chain on one side and a spacered

carboxylic acid on the other. This precursor then served for coupling to mono-, di- and trivalent bipyridine-terminated alcohols using DCC/DPTS as reagents for the esterification reactions to provide the three different ligands in moderate to good yields. The structure of the ligand **83** containing three C_{60} moieties is depicted in Figure 13. On the other hand, large dendritic architecture **82** was constructed for subsequent complexation. This dendrimer **82** consisted of a hexaphenylbenzene core unit, a polarylester fractal part, 24 zinc porphyrins and at the outside relatively small appended polyarylether dendrons to confer solubility to the system. All bipyridines have been demonstrated to strongly bind to the zinc porphyrins with an average binding affinity, as estimated by simply assuming a one-to-one coordination between the individual zinc porphyrin and pyridine units, of 1.2×10^6 M^{-1}. This value was more than two orders of magnitude greater than association constants reported for monodentate coordination between zinc porphyrins and pyridine derivatives and could be ascribed to the simultaneous coordination of two Zn centers of **82** by the two pyridine moieties of for instance **83**. An in-depth study of the photophysical properties of this photactive device mirrored an almost quantitative intramolecular photoinduced electron transfer from the photoexcited porphyrins to the C_{60} units as evidenced by means of steady-state emission spectroscopy and nanosecond flash photolysis measurements. Importantly, the ratio between the rate constants of charge separation and recombination for **[82][81]$_{12}$** was found to be more than an order of magnitude greater than those reported for preceding porphyrin–fullerene supramolecular dyads and triads. The larger number of the C_{60} units in large dendritic architecture **[82][81]$_{12}$** could enhance the probability of electron transfer from the zinc porphyrin units and probably also the opportunity for this electron transfer through efficient energy migration along the densely packed Zn(II) porphyrin array.

Figure 13. Polyporphyrin dendrimer **82** and bipyridine **83** for metal-ligand complexation studies.

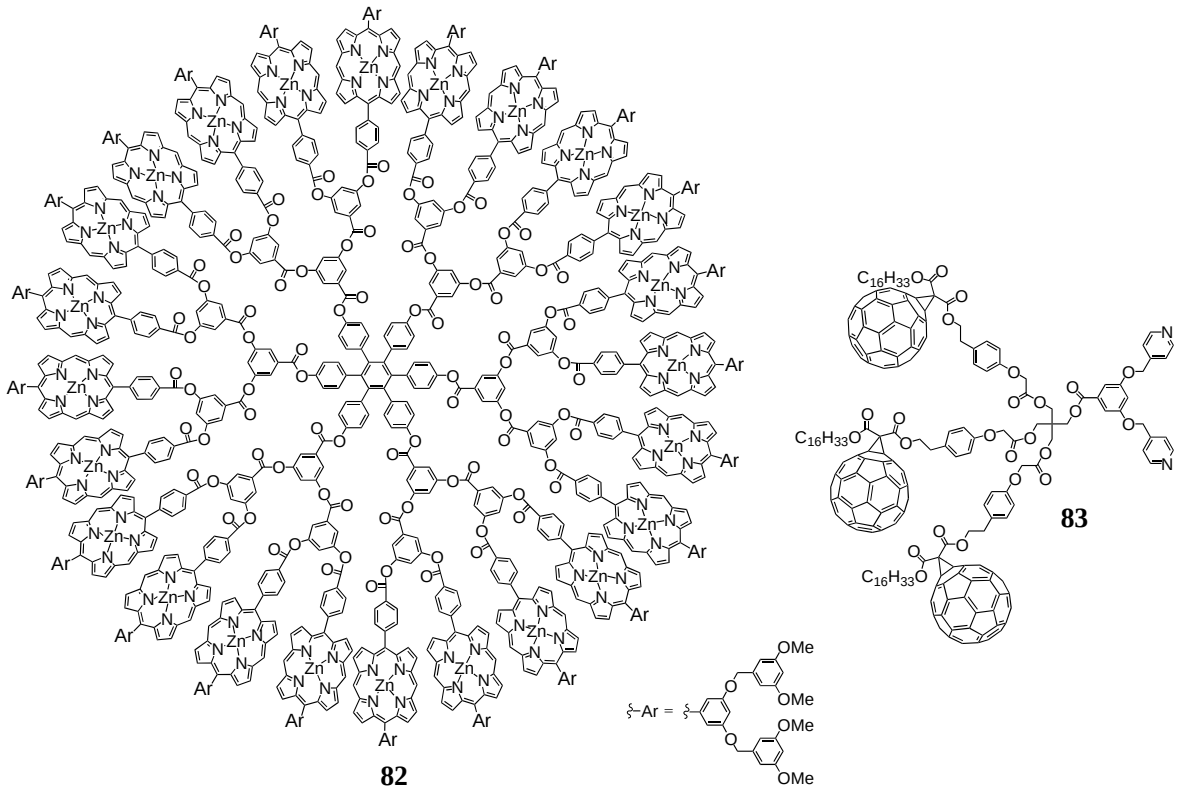

Very recently, large dendrimer architectures with up to 16 porphyrins (the second generation **85** is depicted in Figure 14) discussed before were also engaged in the coordination of fullerene spheres equipped with one pyridine function [55]. According to this, fulleropyrrolidine **84** bearing a pyridine has been obtained upon reaction of C_{60} with *p*-pyridine carboxaldehyde applying Prato conditions. Complexation of the pyridine subunit of fulleropyrrolidine **84** to the multiple zinc porphyrins of for instance **85** led to the supramolecular photoactive dendrimer assemblies. Multiple photosynthetic reaction centers combined with antenna complexes have thus been successfully constructed. The excited energy migration occurs efficiently between porphyrin units followed by charge separation in the supramolecular complex of the largest G3 dendrimer with pyridine-functionalized fulleropyrrolidine **84** as a result of the dendrimer effect. Measuring the charge-separated state of the supramolecular complex produced upon laser excitation had a particular long lifetime of 0.25 ms. Similarly, Ogawa *et al*. exploited the same fulleropyrrolidine **84** for the complexation with zinc porphyrins [56]. Upon the preparation of a π-conjugated porphyrin polymer, this molecular wire has been subjected to the coordination by **84**. The electrical devices fabricated from the two electroactive units showed photo-responsive conduction with a tunneling mechanism at low temperatures and thermionic emission at high temperatures.

Figure 14. Multiple metal-ligand complexation between polyporphyrin dendrimer **85** and fulleropyrrolidine **84**.

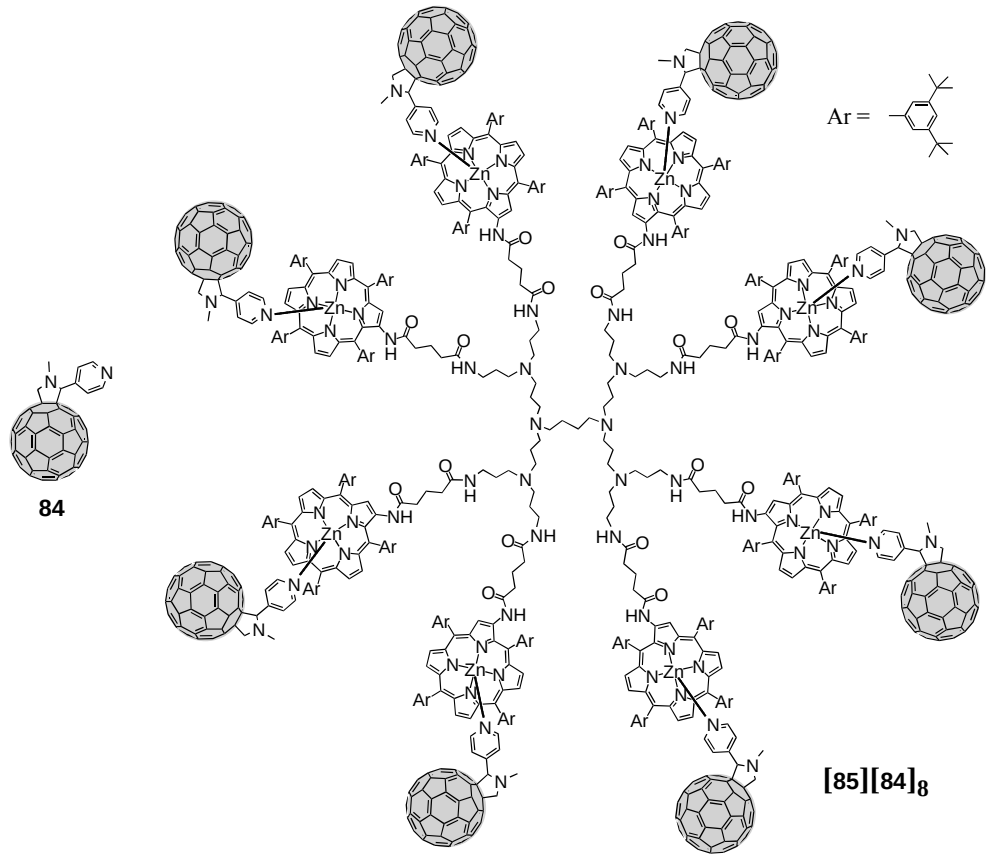

The supramolecular formation of host/guest complexes has also been described by Shinkai *et al*. [57]. They prepared a rigid star-shaped D_3-symmetric receptor that carried six peripheral zinc porphyrin moieties linked through phenylacetylene spacers (Figure 15). This dendritic receptor had three

rotational axes responsible for the spatial arrangement of the porphyrin-derived macrocycles. Addition of C_{60} to a solution containing dendritic host **86** led to the formation of sandwich complexes in an allosteric manner resulting from the tweezering of one fullerene molecule by two zinc porphyrins. The complexation thereby strongly affected the molecular shape as the host-guest complexes suppressed rotational freedom upon formation. Binding studies furthermore evidenced considerably enhanced association constants owing to the binding in a positive allosteric manner.

Figure 15. Rigid star-shaped receptor-fullerene complex [**86**][$\mathbf{C_{60}}$]$_3$.

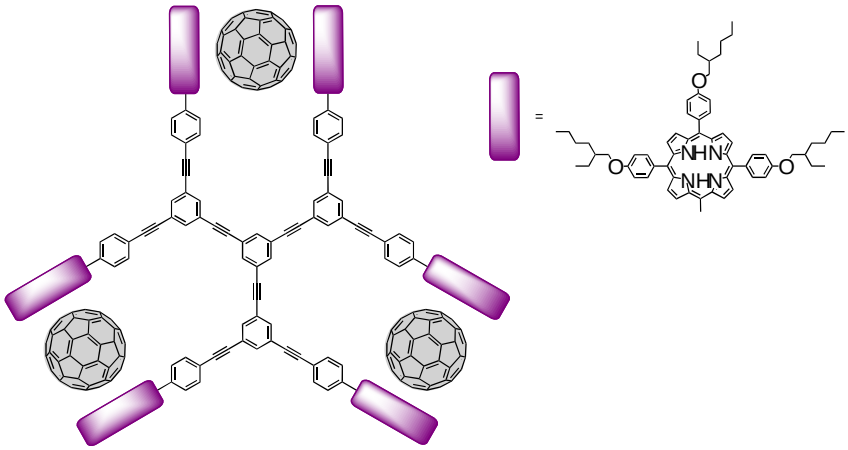

Similarly, a less rigid system has been introduced aiming at the first organic photovoltaic system using supramolecular complexes of porphyrin dendrimers with fullerenes [58–61]. Accordingly, terminal amines of generation one to three POPAM dendrimers have been modified through grafting of porphyrin derivatives endowed with an activated ester. Porphyrin dendrimers **87**-**89** were then employed in the formation of supramolecular assemblies with C_{60} and using an acetonitrile/toluene mixed solvent system led to the clusterization of the nanoscale ensembles (Figure 16). They have then been deposited onto nanostructured SnO_2 electrodes to show an efficient photoresponse in the visible and near-infrared regions, as well as a high photoenergy conversion efficiency due to the effective electron transfer from the excited porphyrin to fullerene within the dendritic matrix.

Márquez *et al*. presented the inclusion of C_{60} molecules within the internal cavities of a fifth generation POPAM dendrimer with 64 terminal amine groups [62]. Following the procedure by Meijer, the product was obtained by adding C_{60} to a solution of a POPAM fifth dendrimer in CH_2Cl_2 and the presence of triethyamine. The resulting mixture was stirred for one day upon which was added *N*-*t*-Boc-L-phenylalanine *N*-hydroxysuccinimide ester as bulky substituent in order to build a protecting shell at the dendrimer surface. After additional stirring for 24 h, the crude has been purified and characterized by MALDI-TOF mass spectrometry and UV-vis spectroscopy. It turned out that the final complex structure [**90**][C_{60}]$_x$ contained an average number of approx. 4 fullerenes that were encapsulated within the dendrimer voids (Figure 17). The dense external shell created with the *N*-*t*-Boc-protected amino acid was thus successfully able to hermetically lock the internal space preventing the trapped fullerene molecules to escape. Interestingly, the fluorescence spectrum revealed that the confinement into a dendritic structure had a noticeable influence on the emission spectra of the guest molecule since under these conditions the emission band of C_{60} experienced a strong

bathochromic shift of *ca*. 132 nm with respect to the emission of C_{60} in solution (λ_{em} = 675 nm after λ_{exc} = 285 nm). This impressive red shift turned out to be solvent-dependent due to favorable electronic communication between host and guest molecules that could be stronger due to the different solvent polarities that significantly affected the macromolecular dendrimer host structure.

Another approach towards supramolecular structures has been introduced by Kono *et al*. [63]. Decoration of the surface of G4-PAMAM dendrimer by *β*-cyclodextrins (*β*-CD) through reaction with the corresponding monotosylated *β*-CD followed by the coupling of monomethoxy polyethylene glycol PEG 4-nitrophenyl carbonate gave the target dendrimer scaffold. ^{1}H NMR studies revealed the average number of bound *β*-CDs to be 29. It is a well-known phenomenon that cyclodextrins form non-covalent associates with fullerenes. For instance, in the case of *β*-CD the ball-shaped C_{60} is encapsulated within two cyclic oligosaccharides. Addition of pristine fullerene led indeed to the proposed host-guest conjugates with concentration reaching values of 2.8 μM aqueous fullerene solutions.

Figure 16. Noncovalent ensembles of C_{60} with first to third generation POPAM dendrimers **87**-**89** decorated at the surface by multiple porphyrin macrocycles.

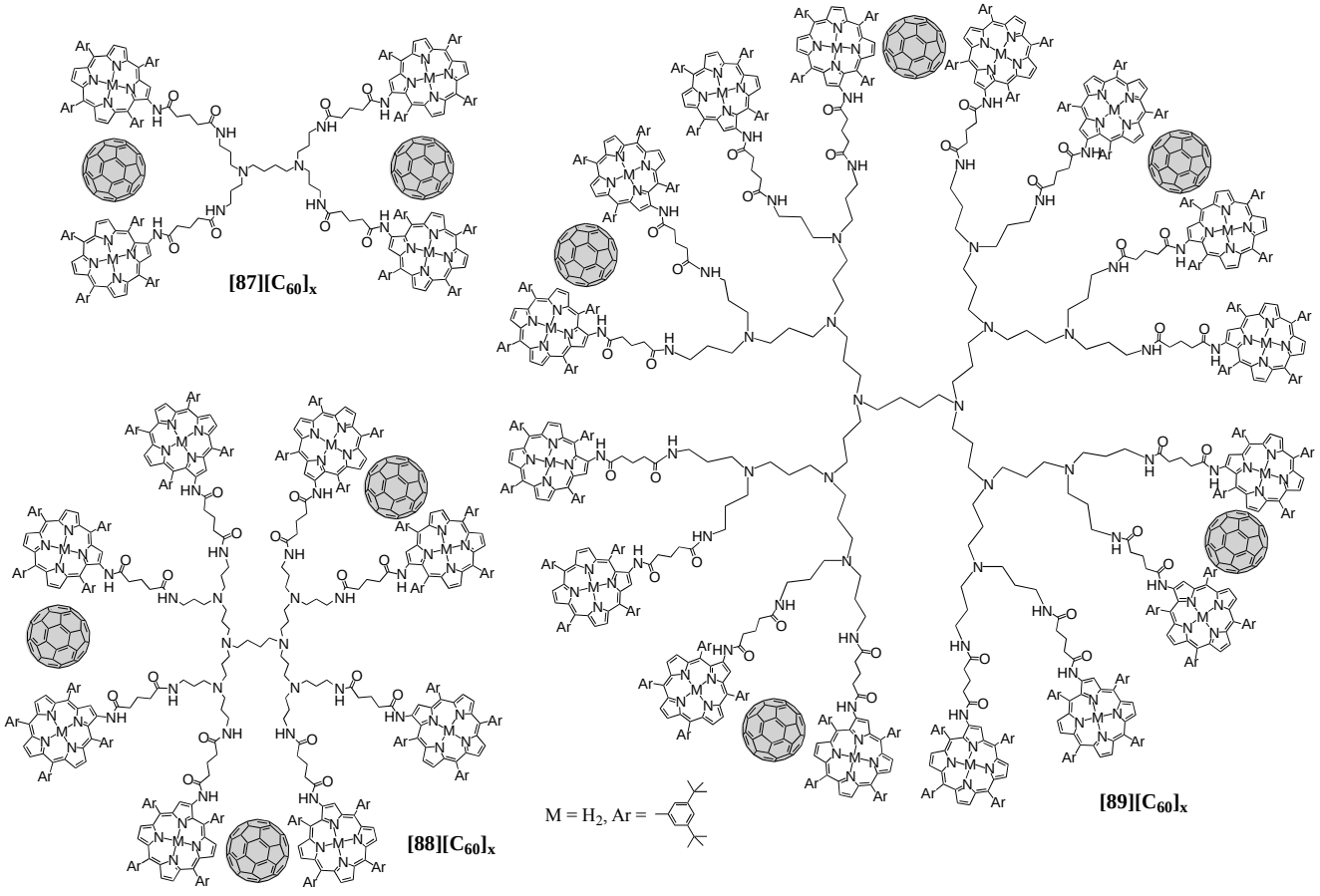

Figure 17. Schematic representation of encapsulated fullerene moieties within the backbone of a POPAM G5 dendrimer according to Márquez *et al* [62].

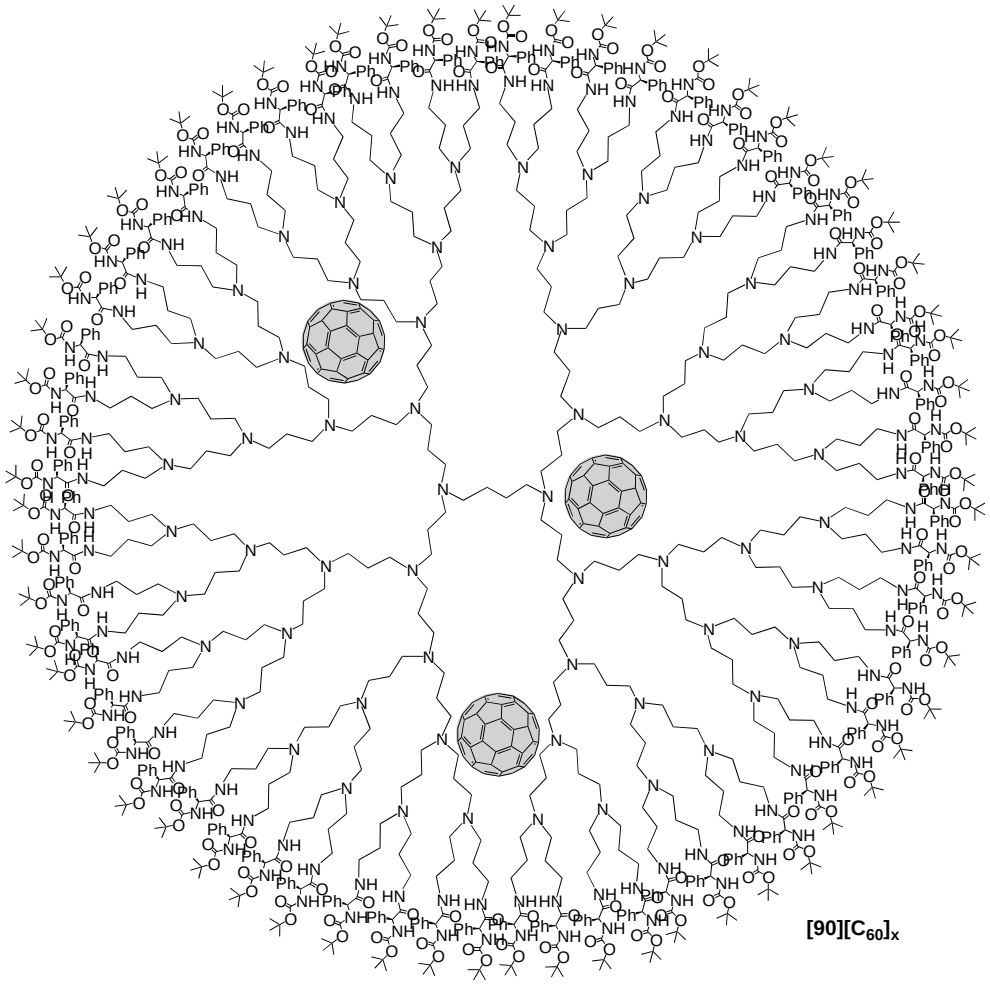

Martín *et al*. also reported the tweezering of fullerene by extended tetrathiafulvalene (ex-TTF) units [64]. The dendrimer skeleton has been prepared employing the general concept of repetitive synthetic sequences to provide the polyester backbone with either 6, 12 (**91**) or 24 ex-TTF moieties at the dendrimer surface. In agreement with previous findings of the same group, tweezering of fullerene was envisaged and indeed, it was found that regardless of the dendrimer size C_{60} could be accommodated. A schematic representation of a possible supramolecular associate of G3 ex-TTF dendrimer 90 and several C_{60} units is depicted in Figure 18. Initial UV/vis titration studies with the first generation species evidenced a positive cooperative binding of three equivalents of C_{60} by the present six ex-TTF units. Similar experiments have then been conducted with the next higher generation structures, which exhibited a similar degree of cooperativity in the binding events. The authors explained the cooperative effect most probably to arise from the need to disassemble the dendrimers prior to complexation of C_{60}.

Figure 18. Supramolecular complexation of C_{60} units at the surface of an ex-TFF appended third generation dendrimer **91**.

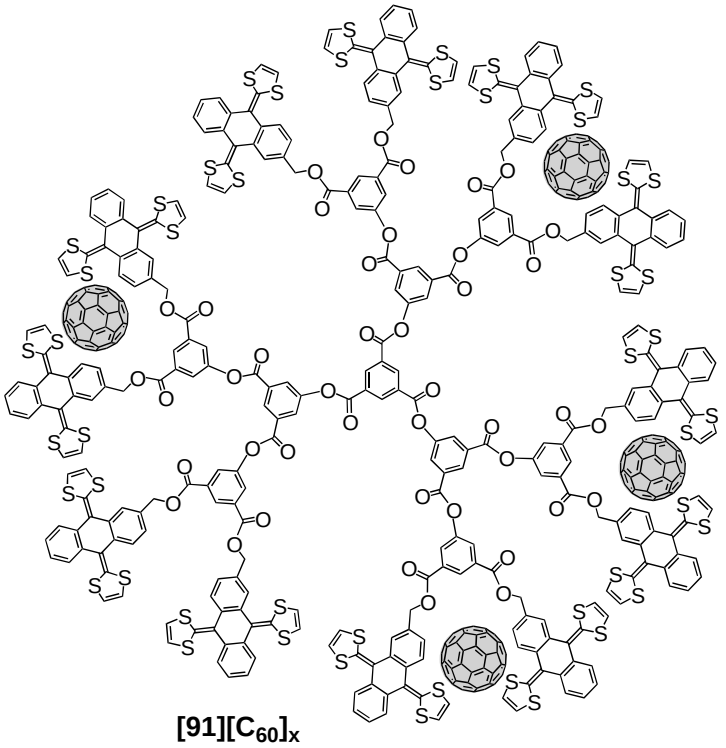

[91][C_{60}]$_x$

6. Conclusions

Since the first specimens of fullerene-containing dendrimers were reported in the early 90s, tremendous efforts have been performed making nowadays accessible a huge variety of new materials with virtually no restriction of dendritic addends that can be linked to the sphere-shaped fullerene molecule. The efficient methodologies that have been developed allow us to attain dendrons with several fullerene moieties in predetermined sites. Most importantly, these synthetic advances in the preparation of fullerodendrimers allow also the tuning of the materials properties to a great extent. The driving force for the steady demand of new materials in chemistry and materials science originates from the peculiar physical properties of this carbon allotrope. It is thus not surprising that the designed fullerodendrons have been incorporated into large dendritic assemblies by either covalent bonds or supramolecular interactions. However, despite the remarkable recent achievements, it is clear that the examples summarized herein do only represent the first steps towards the design of fullerene-rich molecular assemblies which can display functionality at the macroscopic level. More research in this area is clearly required to fully explore the possibilities offered by these materials, for example in nanotechnology or in photovoltaics.

Acknowledgments

The *Centre National de la Recherche Scientifique* and the *University of Strasbourg* (UMR 7509) is gratefully acknowledged for financial support.

References

1. Buhleier, E.; Wehner, W.; Vögtle, F. "Cascade"- and "Nonskid-chain-like" syntheses of molecular cavity topologies. *Synthesis* **1978**, *10*, 155–158.
2. Newkome, G.R.; Moorefield, C.N.; Vögtle, F. *Dendrimers and Dendrons: Concepts, Syntheses, Applications*; VCH: Weinheim, Germany, 2001.
3. Fréchet, J.M.J., Tomalia, D.A., Eds. *Dendrimers and other Dendritic Polymers*; Wiley: Chichester, UK, 2001.
4. Vögtle, F.; Richardt, G.; Werner, N. *Dendrimer Chemistry*; Wiley-VCH: Weinheim, Germany, 2009.
5. Wooley, K.L.; Hawker, C.J.; Frechet, J.M.J.; Wudl, F.; Srdanov, G.; Shi, S.; Li, C.; Kao, M. Fullerene-bound dendrimers—Soluble, isolated carbon clusters. *J. Am. Chem. Soc.* **1993**, *115*, 9836–9837.
6. Nierengarten, J.-F. Fullerodendrimers: A new class of compounds for supramolecular chemistry and materials science applications. *Chem. Eur. J.* **2000**, *6*, 3667–3670.
7. Hirsch, A.; Vostrowsky, O. Dendrimers with carbon-rich cores. *Top. Curr. Chem.* **2001**, *217*, 51–93.
8. Nierengarten, J.-F. Fullerodendrimers: Fullerene-containing macromolecules with intriguing properties. *Top. Curr. Chem.* **2003**, *228*, 87–110.
9. Nierengarten, J.-F. Chemical modification of C_{60} for materials science applications. *New J. Chem*. **2004**, *28*, 1177–1191.
10. Hahn, U.; Cardinali, F.; Nierengarten, J.-F. Supramolecular chemistry for the self-assembly of fullerene-rich dendrimers. *New J. Chem*. **2007**, *31*, 1128–1138.
11. Figueira-Duarte, T.M.; Gégout, A.; Nierengarten, J.-F. Molecular and supramolecular C_{60}-oligophenylenevinylene conjugates. *Chem. Commun*. **2007**, 109–119.
12. Holler, M.; Nierengarten, J.-F. Synthesis and properties of fullerene-rich dendrimers. *Aust. J. Chem*. **2009**, *62*, 605–623.
13. Felder, D.; Gutiérrez-Nava, M.; del Pilar Carreón, M.; Eckert, J.-F.; Luccisano, M.; Schall, C.; Masson, P.; Gallani, J.-L.; Heinrich, B.; Guillon, D.; *et al*. Synthesis of amphiphilic fullerene derivatives and their incorporation in *Langmuir* and *Langmuir-Blodgett* films. *Helv. Chim. Acta* **2002**, *85*, 288–319.
14. Nierengarten, J.-F.; Gramlich, V.; Cardullo, F.; Diederich, F. Regio- and diastereoselective bisfunctionalization of C_{60} and enantioselective synthesis of a C_{60} derivative with a chiral addition pattern. *Angew. Chem. Int. Ed.* **1996**, *35*, 2101–2103.
15. Hahn, U.; Nierengarten, J.F.; Vögtle, F.; Listorti, A.; Monti, F.; Armaroli, N. Fullerene-rich dendrimers: Divergent synthesis and photophysical properties. *New J. Chem.* **2009**, *33*, 337–344.
16. Schenning, A.P.H.J.; Elissen-Román, C.; Weener, J.-W.; Baars, M.W.P.L.; van der Gaast, S.J.; Meijer, E.W. Amphiphilic dendrimers as building blocks in supramolecular assemblies. *J. Am. Chem. Soc.* **1998**, *120*, 8199–8208.
17. Baars, M.W.P.L.; Söntjens, S.H.M.; Fischer, H.M.; Peerlings, H.W.I.; Meijer, E.W. Liquid-crystalline properties of poly(propylene imine) dendrimers functionalized with cyanobiphenyl mesogens at the periphery. *Chem. Eur. J.* **1998**, *4*, 2456–2466.

18. Dirksen, A.; Hahn, U.; Schwanke, F.; Reek, J.N.H.; Williams, R.M.; Vögtle, F.; De Cola, L. Multiple recognition of barbiturate guests by Hamilton-receptor-functionalized dendrimers. *Chem. Eur. J.* **2004**, *10*, 2036–2047.
19. Kim, J.; Yun, M.H.; Lee, J.; Kim, J.Y.; Wudl, F.; Yang, C. A synthetic approach to a fullerene-rich dendron and its linear polymer via ring-opening metathesis polymerization. *Chem. Commun.* **2011**, *47*, 3078–3080.
20. Fiset, E.; Morin, J.F. Synthesis, characterization and modification of azide-containing dendronized diblock copolymers. *Polymer* **2009**, *50*, 1369–1377.
21. Jensen, A.W.; Maru, B.S.; Zhang, X.; Mohanty, D.K.; Fahlman, B.D.; Swanson, D.R.; Tomalia, D.A. Preparation of fullerene-shell dendrimer-core nanoconjugates. *Nano Lett.* **2005**, *5*, 1171–1173.
22. Bustos Bustos, E.; Manríquez Rocha, J.; Echegoyen, L.; Chapman, T.W.; Godínez, L. A. Synthesis and characterization of multilayer films of dendrimer assembled C_{60} materials on nanocrystalline TiO_2 electrodes. *J. Mex. Chem. Soc.* **2007**, *51*, 72–80.
23. Nierengarten, J.-F.; Felder, D.; Nicoud, J.-F. Preparation of dendrons with peripheral fullerene units. *Tetrahedron Lett*. **1999**, *40*, 269–272.
24. Camerano, J.A.; Casado, M.A.; Hahn, U.; Nierengarten, J.-F.; Maisonhaute, E.; Amatore, C. Fullerodendrimers with a tris-isocyanate core allowing their anchoring onto gold surfaces. *New J. Chem.* **2007**, *31*, 1395–1399.
25. Nierengarten, J.-F.; Felder, D.; Nicoud, J.-F. Methanofullerene-functionalized dendritic branches. *Tetrahedron Lett.* **2000**, *41*, 41–44.
26. Trimpin, S.; Keune, S.; Rader, H.J.; Müllen, K. Solvent-free MALDI-MS: Developmental improvements in the reliability and the potential of MALDI in the analysis of synthetic polymers and giant organic molecules. *J. Am. Soc. Mass Spectrom.* **2006**, *17*, 661–671.
27. Felder, D.; Gallani, J.-L.; Guillon, D.; Heinrich, B.; Nicoud, J.-F.; Nierengarten, J.-F. Investigations of thin films with amphiphilic dendrimers bearing peripheral fullerene subunits. *Angew. Chem. Int. Ed.* **2000**, *39*, 201.
28. Hahn, U.; Hosomizu, K.; Imahori, H.; Nierengarten, J.-F. Synthesis of dendritic branches with peripheral fullerene subunits. *Eur. J. Org. Chem.* **2006**, 85–91.
29. Herschbach, H.; Hosomizu, K.; Hahn, U.; Leize, E.; Van Dorsselaer, A.; Imahori, H.; Nierengarten, J.-F. Electrospray mass spectrometry analysis of dendritic branches bearing peripheral fullerene subunits. *Anal. Bioanal. Chem.* **2006**, *386*, 46–51.
30. Hosomizu, K.; Imahori, H.; Hahn, U.; Nierengarten, J.-F.; Listorti, A.; Armaroli, N.; Nemoto, T.; Isoda, S. Dendritic effects on structure and photophysical and photoelectrochemical properties of fullerene dendrimers and their nanoclusters. *J. Phys. Chem. C* **2007**, *111*, 2777–2786.
31. Nierengarten, J.-F.; Eckert, J.-F.; Rio, Y.; Carreon, M.D.; Gallani, J.L.; Guillon, D. Amphiphilic diblock dendrimers: Synthesis and incorporation in Langmuir and Langmuir-Blodgett films. *J. Am. Chem. Soc.* **2001**, *123*, 9743–9748.
32. Gutiérrez-Nava, M.; Accorsi, G.; Masson, P.; Armaroli, N.; Nierengarten, J.-F. Polarity effects on the photophysics of dendrimers with an oligophenylenevinylene core and peripheral fullerene units. *Chem. Eur. J.* **2004**, *10*, 5076–5086.

33. Hahn, U.; Maisonhaute, E.; Amatore, C.; Nierengarten, J.-F. Synthesis and electrochemical properties of fullerene-rich nanoclusters synthesized by cobaltcatalyzed cyclotrimerization of bis(aryl)alkyne fullerodendrimers. *Angew. Chem. Int. Ed.* **2007**, *46*, 951–954.
34. Hahn, U.; Nierengarten, J.-F.; Vögtle, F.; Delavaux-Nicot, B.; Monti, F.; Chiorboli, C.; Armaroli, N. Fullerodendrimers with a perylenediimide core. *New J. Chem.* **2011**, *35*, 2234–2244.
35. Serin, J.M.; Brousmiche, D.W.; Fréchet, J.M.J. A FRET-based ultraviolet to near-infrared frequency converter. *J. Am. Chem. Soc.* **2002**, *124*, 11848–11849.
36. El-Khouly, M.E.; Kang, E.S.; Kay, K.Y.; Choi, C.S.; Aaraki, Y.; Ito, O. Silicon-phthalocyanine-cored fullerene dendrimers: Synthesis and prolonged charge-separated states with dendrimer generations. *Chem. Eur. J.* **2007**, *13*, 2854–2863.
37. Nierengarten, J.-F.; Gramlich, V.; Cardullo, F.; Diederich, F. Regio- and diastereoselective bisfunctionalization of C_{60} and enantioselective synthesis of a C_{60} derivative with a chiral addition pattern. *Angew. Chem. Int. Ed. Engl.* **1996**, *35*, 2101–2103.
38. Witte, P.; Hormann, F.; Hirsch, A. Large di- and heptafullerene polyelectrolytes composed of C_{60} building blocks having a highly symmetrical hexakisaddition pattern. *Chem. Eur. J.* **2009**, *15*, 7423–7433.
39. Hahn, U.; Gégout, A.; Duhayon, C.; Coppel, Y.; Saquet, A.; Nierengarten, J.-F. Self-assembly of fullerene-rich nanostructures with a stannoxane core. *Chem. Commun.* **2007**, 516–518.
40. Delavaux-Nicot, B.; Kaeser, A.; Hahn, U.; Gégout, A.; Brandli, P.-E.; Duhayon, C.; Coppel, Y.; Saquet, A.; Nierengarten, J.-F. Organotin chemistry for the preparation of fullerene-rich nanostructures. *J. Mater. Chem.* **2008**, *18*, 1547–1554.
41. Armaroli, N.; Boudon, C.; Felder, D.; Gisselbrecht, J.-P.; Gross, M.; Marconi, G.; Nicoud, J.-F.; Nierengarten, J.-F.; Vicinelli, V. A copper(I) bis-phenanthroline complex buried in fullerene-functionalized dendritic black boxes. *Angew. Chem. Int. Ed.* **1999**, *38*, 3730–3733.
42. Nierengarten, J.-F.; Felder, D.; Nicoud, J.-F. Phenanthroline ligands substituted with fullerene-functionalized dendritic wedges and their copper(I) complexes. *Tetrahedron Lett.* **1999**, *40*, 273–276.
43. Hahn, U.; González, J.J.; Huerta, E.; Segura, M.; Eckert, J.F.; Cardinali, F.; de Mendoza, J.; Nierengarten, J.-F. A highly directional fourfold hydrogen-bonding motif for supramolecular structures through self-assembly of fullerodendrimers. *Chem. Eur. J.* **2005**, *11*, 6666–6672.
44. Folmer, B.J.B.; Sijbesma, R.P.; Kooijman, H.; Spek, A.L.; Meijer, E.W. Cooperative dynamics in duplexes of stacked hydrogen-bonded moieties. *J. Am. Chem. Soc.* **1999**, *121*, 9001–9007, and references there in.
45. Sijbesma, R.P.; Meijer, E.W. Quadruple hydrogen bonded systems. *Chem. Commun.* **2003**, 5–16.
46. Elhabiri, M.; Trabolsi, A.; Cardinali, F.; Hahn, U.; Albrecht-Gary, A.-M.; Nierengarten, J.-F. Cooperative recognition of C_{60}-ammonium substrates by a ditopic oligophenylenevinylene/crown ether host. *Chem. Eur. J.* **2005**, *11*, 4793–4798.
47. Hahn, U.; Elhabiri, M.; Trabolsi, A.; Herschbach, H.; Leize, E.; Van Dorsselaer, A.; Albrecht-Gary, A.-M.; Nierengarten, J.-F. Supramolecular click chemistry with a bis-ammonium-C_{60} substrate and a ditopic crown ether host. *Angew. Chem. Int. Ed.* **2005**, *44*, 5338–5341.

48. Nierengarten, J.-F.; Hahn, U.; Trabolsi, A.; Herschbach, H.; Cardinali, F.; Elhabiri, M.; Leize, E. Van Dorsselaer, A.; Albrecht-Gary, A.-M. Synthesis of fullerodendrons with an ammonium unit at the focal point and their cooperative self-assembly on a fluorescent ditopic crown ether receptor. *Chem. Eur. J.* **2006**, *12*, 3365–3373.
49. Hager, K.; Hartnagel, U.; Hirsch, A. Supramolecular dendrimers self-assembled from dendritic fullerene ligands and a homotritopic Hamilton receptor. *Eur. J. Org. Chem.* **2007**, 1942–1956.
50. Gnichwitz, J.F.; Wielopolski, M.; Hartnagel, K.; Hartnagel, U.; Guldi, D.M.; Hirsch, A. Cooperativity and tunable excited state deactivation: Modular self-assembly of depsipeptide dendrons on a Hamilton receptor modified porphyrin platform. *J. Am. Chem. Soc.* **2008**, *130*, 8491–8501.
51. Maurer, K.; Grimm, B.; Wessendorf, F.; Hartnagel, K.; Guldi, D.M.; Hirsch, A. Self-assembling depsipeptide dendrimers and dendritic fullerenes with new *cis*- and *trans*-symmetric Hamilton receptor functionalized Zn-porphyrins: Synthesis, photophysical properties and cooperativity phenomena. *Eur. J. Org. Chem.* **2010**, 5010–5029.
52. Ruiz, J.; Pradet, C.; Varret, F.; Astruc, D. Molecular batteries: Synthesis and characterization of a dendritic 19-electron Fe^{I} complex that reduces C_{60} to its mono-anion. *Chem. Commun*. **2002**, 1108–1109.
53. van de Coevering, R.; Kreiter, R.; Cardinali, F.; van Koten, G.; Nierengarten, J.-F.; Klein Gebbink R.J.M. An octa-cationic core-shell dendrimer as a molecular template for the assembly of anionic fullerene derivatives. *Tetrahedron Lett*. **2005**, *46*, 3353–3356.
54. Li, W.S.; Kim, K.S.; Jiang, D.L.; Tanaka, H.; Kawai, T.; Kwon, J.H.; Kim, D.; Aida, T. Construction of segregated arrays of multiple donor and acceptor units using a dendritic scaffold: Remarkable dendrimer effects on photoinduced charge separation. *J. Am. Chem. Soc.* **2006**, *128*, 10527–10532.
55. Fukuzumi, S.; Saito, K.; Ohkubo, K.; Khoury, T.; Kashiwagi, Y.; Absalom, M.A.; Gadde, S.; D'Souza, F.; Araki, Y.; Ito, O.; Crossley, M.J. Multiple photosynthetic reaction centres composed of supramolecular assemblies of zinc porphyrin dendrimers with a fullerene acceptor. *Chem. Commun.* **2011**, *47*, 7980–7982.
56. Kobata, K.; Ogawa, J.; Pandey, S.S.; Oshima, H.; Arai, T.; Kato, T.; Nishino, N. Synthesis and characterization of dendritic poly(L-lysine) containing porphyrin-fullerene moieties. *Synth. Met.* **2007**, *157*, 311–317.
57. Ayabe, M.; Ikeda, A.; Kubo, Y.; Takeuchi, M.; Shinkai, S. A dendritic porphyrin receptor for C_{60} which features a profound positive allosteric effect. *Angew. Chem. Int. Ed.* **2002**, *41*, 2790–2792.
58. Hasobe, T.; Kashiwagi, Y.; Absalom, M.A.; Sly, J.; Hosomizu, K.; Crossley, M.J.; Imahori, H.; Kamat, P.V.; Fukuzumi, S. Supramolecular photovoltaic cells using porphyrin dendrimers and fullerenes. *Adv. Mater.* **2004**, *16*, 975–979.
59. Hasobe, T.; Kamat, P.V.; Absalom, M.A.; Kashiwagi, Y.; Sly, J.; Crossley, M.J.; Hosomizu, K.; Imahori, H.; Fukuzumi, S. Supramolecular photovoltaic cells based on composite molecular nanoclusters: Dendritic porphyrin and C_{60}, porphyrin dimer and C_{60}, and Porphyrin-C_{60} dyad. *J. Phys. Chem. B* **2004**, *108*, 12865–12872.
60. Umeyama, T.; Imahori, H. Self-organization of porphyrins and fullerenes for molecular photoelectrochemical devices. *Photosynth. Res.* **2006**, *87*, 63–71.

61. Fukuzumi, S.; Hasobe, T.; Ohkubo, K.; Crossley, M.J.; Kamat, P.V.; Imahori, H. π-Complex formation in electron-transfer reactions of porphyrins. *J. Porphyrins Phthalocyanines* **2004**, *8*, 191–200.
62. Márquez, F.; Sabater, A.J. Modulation of the photophysical properties of C_{60} by electronic confinement effect. *J. Phys. Chem. A* **2005**, *109*, 1559–1563.
63. Kojima, C.; Toi, Y.; Harada, A.; Kono, K. Aqueous solubilization of fullerenes using poly(amidoamine) dendrimers bearing cyclodextrin and poly(ethylene glycol). *Bioconjug. Chem.* **2008**, *19*, 2280–2284.
64. Fernández, G.; Sánchez, L.; Pérez, E.M.; Martín, N. Large exTTF-based dendrimers. Self-assembly and peripheral cooperative multiencapsulation of C_{60}. *J. Am. Chem. Soc.* **2008**, *130*, 10674–10683.